ARCHIVIO ISTITUZIONALE DELLA RICERCA

Alma Mater Studiorum Università di Bologna
Archivio istituzionale della ricerca

Validity of the Diplostomoidea and Diplostomida (Digenea, Platyhelminthes) upheld in phylogenomic analysis

This is the submitted version (pre peer-review, preprint) of the following publication:

Published Version:
Locke, S.A., Van Dam, A., Caffara, M., Pinto, H.A., López-Hernández, D., Blanar, C.A. (2018). Validity of the Diplostomoidea and Diplostomida (Digenea, Platyhelminthes) upheld in phylogenomic analysis. INTERNATIONAL JOURNAL FOR PARASITOLOGY, 48(13), 1043-1059 [10.1016/j.ijpara.2018.07.001].

Availability:
This version is available at: https://hdl.handle.net/11585/661036 since: 2021-12-15

Published:

DOI: http://doi.org/10.1016/j.ijpara.2018.07.001

Terms of use:

Some rights reserved. The terms and conditions for the reuse of this version of the manuscript are specified in the publishing policy. For all terms of use and more information see the publisher's website.

This item was downloaded from IRIS Università di Bologna (https://cris.unibo.it/).
When citing, please refer to the published version.

(Article begins on next page)

16 July 2024

bioRxiv preprint doi: https://doi.org/10.1101/333518; this version posted May 30, 2018. The copyright holder for this preprint (which was not certified by peer review) is the author/funder, who has granted bioRxiv a license to display the preprint in perpetuity. It is made available under aCC-BY 4.0 International license.

Title: Nuclear and mitochondrial phylogenomics of the Diplostomoidea and Diplostomida (Digenea, Platyhelminthes)[1]

Authors: Sean A. Locke[a,*], Alex Van Dam[a], Monica Caffara[b], Hudson Alves Pinto[c], Danimar López-Hernández[c], Christopher Blanar[d]

[a]University of Puerto Rico at Mayagüez, Department of Biology, Box 9000, Mayagüez, Puerto Rico 00681–9000

[b]Department of Veterinary Medical Sciences, Alma Mater Studiorum University of Bologna, Via Tolara di Sopra 50, 40064 Ozzano Emilia (BO), Italy

[c]Departament of Parasitology, Instituto de Ciências Biológicas, Universidade Federal de Minas Gerais, Belo Horizonte, Minas Gerais, Brazil.

[d]Nova Southeastern University, 3301 College Avenue, Fort Lauderdale, Florida, USA 33314-7796.

[*]corresponding author: University of Puerto Rico at Mayagüez, Department of Biology, Box 9000, Mayagüez, Puerto Rico 00681–9000. Tel:. +1 787 832 4040x2019; fax +1 787 265 3837.

Email sean.locke@upr.edu

[1] Note: Nucleotide sequence data reported in this paper will be available in the GenBank™ and EMBL databases, and accession numbers will be provided by the time this manuscript goes to press.

bioRxiv preprint doi: https://doi.org/10.1101/333518; this version posted May 30, 2018. The copyright holder for this preprint (which was not certified by peer review) is the author/funder, who has granted bioRxiv a license to display the preprint in perpetuity. It is made available under aCC-BY 4.0 International license.

Abstract: Higher systematics within the Digenea, Carus 1863 have been relatively stable since a phylogenetic analysis of partial nuclear ribosomal markers (rDNA) led to the erection of the Diplostomida Olson, Cribb, Tkach, Bray, and Littlewood, 2003. However, recent mitochondrial (mt) genome phylogenies suggest this order might be paraphyletic. These analyses show members of two diplostomidan superfamilies are more closely related to the Plagiorchiida La Rue, 1957 than to other members of the Diplostomida. In one of the groups implicated, the Diplostomoidea Poirier, 1886, a recent phylogeny based on mt DNA also indicates the superfamily as a whole is non-monophyletic. To determine if these results were robust to additional taxon sampling, we analyzed mt genomes from seven diplostomoids in three families. To choose between phylogenetic alternatives based on mt genomes and the prior rDNA-based topology, we also analyzed hundreds of ultra-conserved elements (UCEs) assembled from shotgun sequencing. The Diplostomida was paraphyletic in the mt genome phylogeny, but supported in the UCE phylogeny. We speculate this mitonuclear discordance is related to ancient, rapid radiation in the Digenea. Both UCEs and mt genomes support the monophyly of the Diplostomoidea and show congruent relationships within it. The Cyathocotylidae Mühling, 1898 are early diverging descendants of a paraphyletic clade of Diplostomidae Poirier, 1886, in which were nested members of the Strigeidae Railliet, 1919; the results support prior suggestions that the Crassiphialinae Sudarikov, 1960 will rise to the family level. Morphological traits of diplostomoid metacercariae appear to be more useful for differentiating higher taxa than those of adults. We describe a new species of *Cotylurus* Szidat, 1928, resurrect a species of *Hysteromorpha* Lutz, 1931, and find support for a species of *Alaria* Schrank, 1788 of contested validity. Complete rDNA operons are provided as a resource for future studies.

bioRxiv preprint doi: https://doi.org/10.1101/333518; this version posted May 30, 2018. The copyright holder for this preprint (which was not certified by peer review) is the author/funder, who has granted bioRxiv a license to display the preprint in perpetuity. It is made available under aCC-BY 4.0 International license.

38 **Keywords**: Strigeida, Diplostomida, Phylogenomics, Metacercaria, Nuclear-mitochondrial

39 discordance, *Cotylurus*, *Hysteromorpha*, *Alaria*

40

bioRxiv preprint doi: https://doi.org/10.1101/333518; this version posted May 30, 2018. The copyright holder for this preprint (which was not certified by peer review) is the author/funder, who has granted bioRxiv a license to display the preprint in perpetuity. It is made available under aCC-BY 4.0 International license.

1. Introduction

Early efforts to organize the higher taxonomy of digenetic trematodes relied mainly on external morphology of adults (reviewed by La Rue, 1957). As life cycles became better known, Cort (1917), Stunkard (1946) and others increasingly emphasized other characters, particularly cercarial morphology. Using a variety of methods, different authors produced conflicting hypotheses and higher classifications, but many concluded a close relationship exists among members of the Diplostomoidea Poirier, 1886, the Clinostomatoidea Lühe, 1901, and the Schistosomatoidea Stiles and Hassall, 1898 (Brooks et al., 1985; Dubois, 1970a; Gibson, 1996; La Rue, 1957; Pearson, 1972). Most authors assigned these and other superfamilies to the Strigeida (=Strigeatoidea) La Rue 1957, which are characterized by furcocercous cercariae that penetrate hosts (Gibson and Bray, 1994). The close relationship among strigeids, clinostomes and schistosomes was supported by a phylogenetic analysis of partial nuclear ribosomal markers (rDNA) from digeneans in 77 families (Olson et al., 2003). In this analysis, however, several other families in the Strigeida fell within the Plagiorchiida La Rue, 1957, leading Olson et al. (2003) to erect the order Diplostomida, which now includes diplostomoids, clinostomatids, and schistosomatoids.

The work of Olson et al. (2003) created stability in higher systematics within the Digenea. For example, the subsequent studies and future research directions discussed by Kostadinova and Pérez-del-Olmo (2014) are mainly limited to intra-ordinal relationships. However, recent work raises questions about the status of the Diplostomida (Fig. 1). Separate phylogenetic analyses of mt genomes show two diplostomidans (*Clinostomum* Leidy, 1856, *Diplostomum* von Nordmann, 1832) are more closely related to the Plagiorchiida than to other members of the Diplostomida (Brabec et al., 2015; Briscoe et al., 2016; Chen et al., 2016; see also Fig. 5 in Park, 2007). Brabec

bioRxiv preprint doi: https://doi.org/10.1101/333518; this version posted May 30, 2018. The copyright holder for this preprint (which was not certified by peer review) is the author/funder, who has granted bioRxiv a license to display the preprint in perpetuity. It is made available under aCC-BY 4.0 International license.

et al. (2015) argued that data from additional taxa are needed before biological and taxonomic implications can be judged. However, it is well to note that the mt phylogenies were based on alignments of considerably more characters than the rDNA phylogeny of Olson et al. (2003). Moreover, mt genome analyses now collectively include two of three diplostomidan superfamilies, and statistical support for the alliance of non-schistosome diplostomidans with the Plagiorchiida has increased with increased taxon sampling (support of the key nodes of 0.77 in Brabec et al., 2015; 1.0 in Chen et al., 2016; 0.93 in Briscoe et al., 2016). More generally, mtDNA has been useful in revealing ordinal relationships in other Platyhelminthes (Waeschenbach et al., 2012). Further evaluation of this discordance (Fig. 1) was one of two goals of our study.

Another was to estimate relationships among members of one superfamily in the Diplostomida, the Diplostomoidea, which are characterized by the tribocytic organ, a holdfast absent in other digeneans. Six families recognized or erected by Dubois (1938, 1970b) are in wide use, although problems with these classifications are often noted. Shoop's (1989) cladistic analysis indicated the Diplostomidae Poirier, 1886 was paraphyletic. Both Shoop (1989) and Niewiadomska (2002a) agreed that the morphological type of the metacercaria appears to reflect higher relationships in the Diplostomoidea, but the higher classifications of Dubois (1938, 1970b), based largely on the class of hosts and morphology adults, did not take this into account. Most molecular phylogenetic studies indicate the superfamily is monophyletic, but find the two largest families, the Strigeidae Railliet, 1919 and Diplostomidae, are not (Blasco-Costa and Locke, 2017; Dzikowski et al., 2004; Olson et al., 2003). One analysis of partial cytochrome *c* oxidase 1 (CO1) recovered the Cyathocotylidae Mühling, 1898 (Diplostomoidea) within the

bioRxiv preprint doi: https://doi.org/10.1101/333518; this version posted May 30, 2018. The copyright holder for this preprint (which was not certified by peer review) is the author/funder, who has granted bioRxiv a license to display the preprint in perpetuity. It is made available under aCC-BY 4.0 International license.

Schistosomatoidea (Hernández-Mena et al., 2017), which suggests even the superfamily could be non-monophyletic.

Two obstacles currently prevent molecular assessment of higher taxonomy within the Diplostomoidea, its position within the Digenea, and implications for the order Diplostomida. The first is poor taxonomic and geographic coverage (Blasco-Costa and Locke, 2017). Recent work is encouraging, with studies including members of the Proterodiplostomidae Dubois, 1936 (Hernández-Mena et al., 2017), Brauninidae Wolf, 1903 and Cyathocotylidae (Blasco-Costa and Locke, 2017; Fraija-Fernández et al., 2015), and less well-sampled regions (Blasco-Costa et al., 2016; Chaudhary et al., 2017; López-Hernández et al., 2018; Sereno-Uribe et al., 2018).

Another issue is that accumulating molecular data may not be sufficiently rich in characters to resolve higher relationships. Most analyses of intra-diplostomoid relations are based on sequences of DNA from one or two loci totalling less than 2000 bp in length (e.g., Blasco-Costa and Locke, 2017, and references therein). This seems sufficient for specimen identification, discrimination of species, and species membership in genera (e.g., Chibwana et al. 2013; Locke et al. 2015; López-Hernández et al., 2018), but relationships among genera and families are less resolved. For example, there is inconsistency and often little support in the polarity among *Alaria*, *Apharyngostrigea,* and *Cardiocephaloides* in fig. 3 in Olson et al. (2003), fig. 1 in Fraija-Fernández et al. (2015), and fig. 2 in Hernández-Mena et al. (2017), which are all phylogenies based on concatenated sequences of rDNA subunits. The deep conflict between recent mt genome phylogenies and those based on shorter nuclear DNA sequences (Fig. 1) may also be related to differences in the number of informative characters.

Here we attempt to progress on both fronts. We increase the number and diversity of mitochondrial genomes from the Diplostomoidea, in order to explore discordant results of recent

bioRxiv preprint doi: https://doi.org/10.1101/333518; this version posted May 30, 2018. The copyright holder for this preprint (which was not certified by peer review) is the author/funder, who has granted bioRxiv a license to display the preprint in perpetuity. It is made available under aCC-BY 4.0 International license.

phylogenetic studies, namely the possible placement of the Cyathocotylidae outside the Diplostomoidea (Hernández-Mena et al., 2017), and the Diplostomidae as a basal lineage in the order Plagiorchiida (Brabec et al., 2015). Both results originate from analysis of mtDNA, and we obtained data to determine if these patterns were robust to additional taxon sampling. To decide between what were likely to be conflicting topologies based on mtDNA and rDNA, we employed phylogenomic analyses of ultra-conserved elements (UCEs).

Although we set out to work on higher relationships among a small number of representative specimens, we were aware that the diversity and identity of diplostomoid species often differs from initial suspicions based on morphology (Blasco-Costa and Locke, 2017). We therefore supported our identifications with morphological comparisons and analysis of additional DNA sequences from closely related species, which led to several findings related to the alpha taxonomy of the seven specimens of principal interest.

2. Materials and Methods

2.1 Specimen collection and identification

Twenty-five specimens in good condition were selected for potential Illumina shotgun sequencing (described below). These worms had been stored in ethanol and identified to genus, and were chosen to represent major clades in Blasco-Costa and Locke (2017). DNA was extracted from individual worms, or subsamples, using Qiagen's DNEasy blood and tissue kit (GmbH, Germany), following the manufacturer's protocol with two 200-µL elutions. Of these 25 worms, we selected seven (Table 1) after measuring DNA concentration with Nano-drop (0.5-22 ng/µl in 400 µl) and Qubit (0-4.96 ng/µl) and excluding samples with evidence of DNA degradation (Bioanalyzer).

bioRxiv preprint doi: https://doi.org/10.1101/333518; this version posted May 30, 2018. The copyright holder for this preprint (which was not certified by peer review) is the author/funder, who has granted bioRxiv a license to display the preprint in perpetuity. It is made available under aCC-BY 4.0 International license.

Additional conspecific or closely related parasites that contributed to identification of the seven worms, or constituted relevant host or geographic records, were processed morphologically and with PCR and Sanger sequencing (see below). Morphological vouchers were cleared in Amman's lactophenol, rehydrated, stained in dilute acetocarmine, dehydrated in ethanol, cleared in clove oil, and mounted on a slide in Canada balsam. Vouchers comprised hologenophores (DNA sequenced from the worm studied morphologically), paragenophores (similar worms from the same individual host paired for either morphological or molecular work) and syngenophores (voucher worms from different host individuals collected at the same time, or on other occasions, or in the same region, as the worms from which DNA was extracted) (Pleijel et al., 2008). Drawings and measurements were made with the aid of a camera lucida and ocular micrometer.

2.2 Molecular and phylogenetic analysis

Seven samples were processed on a single lane of an Illumina HiSeq 4000 and 150-bp paired-end libraries were built using Illumina TrueSeq adapters at the UC Davis Genome Center. Partial CO1 barcodes were obtained using the primers and PCR protocols of Moszczynska et al. (2009) and Sanger sequencing, from the seven worms or other representatives, and were used to seed iterative assemblies of Illumina reads of whole mitochondrial genomes, using Geneious V9. Mitochondrial genomes were annotated in MITOS (Bernt et al., 2013) using NCBI's Echinoderm and Flatworm Mitochondrial translation table (number 9). Additional annotations, including minor modifications to MITOS output, were made using alignments with mitochondrial genomes from two species of *Diplostomum* (Brabec et al., 2015) (KR269763-4), *Clinostomum complanatum* (KM923964), *Fasciola hepatica* (NC_002546.1), *Trichobilharia regenti* (NC_009680.1), and *Schistosoma japonicum* (NC_002544.1). A similar approach was taken to

bioRxiv preprint doi: https://doi.org/10.1101/333518; this version posted May 30, 2018. The copyright holder for this preprint (which was not certified by peer review) is the author/funder, who has granted bioRxiv a license to display the preprint in perpetuity. It is made available under aCC-BY 4.0 International license.

assemble complete rDNA operons (18S, ITS1, 5.8S, ITS2, and 28S). Illumina reads were mapped to rDNA sequences from, in some cases, the same samples or other representatives obtained using primers in Galazzo et al. (2002); Olson et al. (2003), and in other cases, using previously published sequences from the same species or close relatives (GB ACCESSIONS XXXXXX).

The seven mitochondrial genomes were analyzed with previously published data from Digenea and Eucestoda. Protein-coding regions were extracted and placed in the same order (i.e., atp6+nad2 and nad3 were placed before and after nad1, respectively in *Schistosoma haematobium*, *S. spindale*, and *S. mansoni*, in which the order of these genes differs). Protein-coding regions were concatenated, and both nucleotide and translated into amino acid sequences were aligned using MAFFT (L-INS-I). Alignments were stripped of columns with gaps and analyzed with RAXML (Silvestro and Michalak, 2012; Stamatakis, 2014) using a substitution model selected with the Bayesian Information Criterion (Tamura et al., 2013).

For UCE work, quality trimming was conducted with bbduk from the BBMap package (Bushnell, 2014). *De novo* genomes were assembled for each sample with IDBA-Hybrid (Peng et al., 2012) using *Schistosoma mansoni* (GCF_000237925.1) to help scaffold similar regions. The quality of *de novo* assemblies was assessed with BUSCO (Simão et al., 2015). Conserved genomic regions across were identified using PHYLUCE v1.6 (Faircloth, 2016). Trimmed reads were aligned to the *S. mansoni* genome using stampy-1.0 (Lunter and Goodson, 2011) with a substitution rate set to 0.05 to capture overlapping regions with trimmed data. Using overlapping regions from the *S. mansoni* genome, an initial probe set was mapped back to the *de novo* genomes via PHYLUCE scripts. Genomes were similarly analyzed from *Clonorchis sinensis*

bioRxiv preprint doi: https://doi.org/10.1101/333518; this version posted May 30, 2018. The copyright holder for this preprint (which was not certified by peer review) is the author/funder, who has granted bioRxiv a license to display the preprint in perpetuity. It is made available under aCC-BY 4.0 International license.

(PRJDA72781), *Echinostoma caproni* (PRJEB1207), *Diphyllobothrium latum* (PRJEB1206), and *Fasciola hepatica* (PRJEB6687).

Complete probe sets were generated for ten out of twelve species (phyluce_probe_query_multi_fasta_table in PHYLUCE), with 801 loci and 16,671 3 × tiling probes post-duplicate-filtering. Loci were aligned using MAFFT and with 90% matrix occupancy, 517 loci were retained. The MAFFT-Gblocks option was called in PHYLUCE to remove poorly aligned regions. Phylogenetic reconstructions were computed using RAxML (Stamatakis, 2014) from a concatenated matrix with GTRGAMMA substitution rate, with 1,000 bootstrap replicates in each of 20 parallel runs, and *Diphyllobothrium latum* set as outgroup. The resulting maximum-likelihood (ML) tree with bootstrap bi-partitions was annotated with morphological and life-history characters from the Diplostomoidea (supplementary Fig. 1). We also generated one tree without setting *D. latum* as the outgroup, and another after running PHYLUCE and RAxML solely with the seven diplostomoids and *S. mansoni* set as outgroup (the latter yielding 796 conserved genetic elements, and 63,959 variable sites based on 85% matrix occupancy). In both the latter cases (not shown), the topology obtained was well supported and indistinguishable from the UCE tree reported below.

3. Results

3.1 General molecular results

The genomic analysis of seven samples yielded 7.8×10^8 150-bp reads, mean 1.1×10^8, range 2.1×10^7–1.4×10^8 reads per sample; mean N50=2833 bp, range 542-11122 bp). Below, and in Table 2, these and other results are broken down by species.

3.2 Phylogenetic analysis of mitochondrial genomes

bioRxiv preprint doi: https://doi.org/10.1101/333518; this version posted May 30, 2018. The copyright holder for this preprint (which was not certified by peer review) is the author/funder, who has granted bioRxiv a license to display the preprint in perpetuity. It is made available under aCC-BY 4.0 International license.

The mitochondrial genomes were 13,665 – 15,107 bp in length (supplementary Table 1). The 12 coding regions occurred in the same order as in digeneans other than *S. haematobium*, *S. spindale*, and *S. mansoni*. In *C. prussica*, two pairs of tRNA genes were reversed in order compared with other diplostomoids. One of these reversals, the occurrence of trnN prior to trnP, is also a feature of *Clinostomum complanatum* (KM923964). The order of three tRNA genes occurring between *nad6* and *nad5* in *C. medioconiger* differed from that seen in other diplostomoids, and these genes were positioned adjacent to a 774-bp non-coding span which, among diplostomoids and *Clinostomum*, was unique to *C. medioconiger*.

Phylogenetic analysis of nucleotide or translated amino acid sequences from the 12 concatenated coding regions of the mitochondrial genomes did not support the order Diplostomida (Fig. 2). The diplostomoids and *Clinostomum* emerged as early diverging descendants from common ancestors of the Plagiorchiida, rather than grouping with *Schistosoma* and *Trichobilharzia*.

3.3 Phylogenetic analysis of ultra-conserved elements (UCEs)

The Diplostomoidea were monophyletic in the topology obtained from ML analysis of 517 conserved genetic elements, comprising 84,902 distinct patterns across 234,783 characters per taxon (Fig. 3). Consistent with the concept of the Diplostomida and Plagiorchiida, the Diplostomoidea and *Schistosoma* formed a clade separate from a clade comprising plagiorchiidans *Clonorchis*, *Echinostoma*, and *Fasciola*.

Relationships among diplostomoids were similar to those recovered by analysis of mt genomes, differing slightly within a clade of Diplostominae *Alaria* + *Hysteromorpha* + *Tylodelphys* + *Diplostomum* (Figs. 2, 3). Within the diplostomoids, *Cyathocotyle prussica* was basal to a clade

bioRxiv preprint doi: https://doi.org/10.1101/333518; this version posted May 30, 2018. The copyright holder for this preprint (which was not certified by peer review) is the author/funder, who has granted bioRxiv a license to display the preprint in perpetuity. It is made available under aCC-BY 4.0 International license.

220 in which the Diplostomidae were paraphyletic. The diplostomid *Posthodiplostomum centrarchi*
221 was basal to a clade of both strigeids and other diplostomids. The two strigeids were sister taxa.

222 The non-molecular characters of metacercariae showed higher correspondence with the UCE
223 topology than did the characters of adults (Fig 3, supplementary Fig. 1). Within the
224 Diplostomoidea all five morphological or life-history characters of metacercariae mapped onto
225 genomic clades, while correspondence was poorer for adult characters. Metacercarial
226 apomorphic characters included the structure of the reserve bladder, presence or absence of
227 encystment, free or enclosed limebodies, and the presence or absence of pseudosuckers, which
228 distinguished clades comprising relatively small subsets of species. For example, the structure of
229 the reserve bladder differs among the following four groups, which correspond to clades in the
230 molecular phylogeny: *Cyathocotyle*, *Posthodiplostomum*, *Cardiocephaloides* + *Cotylurus*, and
231 *Alaria* + *Hysteromorpha* + *Tylodelphys*. Commonly recognized metacercarial morphotypes
232 (prohemistomulum, neascus, tetracotyle, diplostomulum) mapped onto all clades formed.

233 *3.4 Morphological and molecular support of identification or description of species*

234 Specimens were identified morphologically, and dimensions are reported in μm and given as
235 range (means, ±standard deviation, n measured). Sequences of partial sequences of cytochrome *c*
236 oxidase 1 (DNA barcodes) from mitochondrial genomes were also compared to previously
237 published data and with sequences from additional collections. In a neighbour-joining
238 phenogram (Fig. 4), CO1 sequences fell into distinct clusters in which the minimum p-distance
239 between nearest neighbour species was in all cases less than the maximum distance within
240 species; these clusters formed well supported clades in separate ML analysis. Complete rDNA
241 operons (Supplementary Table 1) were subjected to BLAST searches, which supported
242 identifications in all cases, as described further below.

bioRxiv preprint doi: https://doi.org/10.1101/333518; this version posted May 30, 2018. The copyright holder for this preprint (which was not certified by peer review) is the author/funder, who has granted bioRxiv a license to display the preprint in perpetuity. It is made available under aCC-BY 4.0 International license.

243 *3.4.1 Cyathocotyle prussica* Mühling, 1896

244 *Cyathocotyle prussica* was identified based on morphology of the unstained specimen prior to
245 DNA extraction, and its provenance (host, geographic origin). Metacercariae of *C. prussica* have
246 been reported from *Gasterosteus aculeatus* and other small-bodied fishes throughout Europe
247 (Kalbe et al., 2016; Kvach et al., 2016). The DNA used for genomic work was obtained from a
248 metacercaria from *Gasterosteus aculeatus* collected at the same time as the specimen sequenced
249 by Blasco-Costa and Locke (2017) and no morphological voucher remains. The CO1 region of
250 the mitochondrial genome assembly was 99.7 % (587 / 589 identities) similar to MF124273, and
251 the rDNA operon 99.1 % (762/769 identities) similar to KY951726, both from Blasco-Costa and
252 Locke (2017). The rDNA operon differed by 2.5-20.8% from 13 published rDNA sequences
253 from cyathocotylids on GenBank.

254 *3.4.2 Posthodiplostomum centrarchi* (Hoffman, 1958) Stoyanov, Georgieva, Pankov, Kudlai,
255 Kostadinova, and Georgiev, 2017 (Fig. 5).

256 [Measurements from 9 specimens (6 paragenophores, 3 hologenophores) ex *Ardea herodias*,
257 Montreal, Quebec, Canada]

258 Total length 1222–1775; forebody and hindbody separated by marked constriction. Forebody
259 spatulate 680–1200 long, 452–875 wide, oval to lanceolate, with anterior lateral edges often
260 recurved ventrally. Hindbody oval, widest in anterior half, tapering posteriorly, 520–875 long,
261 248–750 wide. Hindbody length / forebody length 0.58–0.86. Oral sucker terminal, 38–72 × 38–
262 72. Ventral sucker 55–90 × 55–80, in posterior half of forebody, centered 54–71 % along
263 forebody sagittal axis. Tribocytic organ 140–200 × 144–256. Pharynx 40–53 long, 40–53 wide.
264 Oesophagus 60–72 long. Ovary lateral to anterior testis at anterior margin of hindbody, 80–105 ×

bioRxiv preprint doi: https://doi.org/10.1101/333518; this version posted May 30, 2018. The copyright holder for this preprint (which was not certified by peer review) is the author/funder, who has granted bioRxiv a license to display the preprint in perpetuity. It is made available under aCC-BY 4.0 International license.

72–88. Testes occupying first 55–80% of hindbody. Anterior testis irregularly, smoothly lobed 96–200 long, 144–272 wide. Posterior testis, sinuous, v-shaped, pointed posteriorly, 176–350 long, 216–350 wide. Vitelline reservoir intertesticular, median. Vitellaria densest at level of posterior of tribocytic organ and in base of forebody, extending anteriorly beyond ventral sucker by slightly more than one ventral-sucker length, in hindbody extending more than halfway to posterior extremity and bifurcating into two posteriorly oriented bands at and beyond vitelline reservoir, sometimes exceeding, sometimes exceeded by, posterior extent of posterior testis. Copulatory bursa eversible, terminal or slightly dorsal, 120–216 long, 135–300 wide, housing muscular genital cone. Eggs few, 0–4, length 70–98 × 42–64 (See supplementary Table 2 for means, standard deviations, n structures measured).

3.4.2.1 Remarks

MacCallum (1921) summarily described *Posthodiplostomum* (*Diplostomum*) *minimum* from *Ardea herodias* in New York, USA. Hoffman (1958) created two sub-species, *P. minimum centrarchi* and *P. minimum minimum*, for lineages infecting either centrarchids or cyprinids, respectively. Stoyanov et al. (2017) elevated the centrarchid subspecies to *P. centrarchi.*

Our observations largely agree with Dubois' (1970b) description of the adult (although he did not distinguish *P. centrarchi* and *P. minimum*), except in the following respects (Supplementary Table 2): Two of nine specimens were up to 75 greater in total length; in 4/9 specimens, we observed the hindbody to be widest at the anterior testis (e.g., Fig 5), rather than at the level of the posterior testis as in Dubois (1970b). The oral sucker was the same length as the pharynx in 1/6 specimens, rather than larger as in Dubois (1970b); the tribocytic organ was wider in 3/6 specimens (200-256 *versus* maximum of 190 in Dubois, 1970b); and in 7/9 specimens the copulatory bursa was both longer and wider than maximum values (160 × 160) reported by

bioRxiv preprint doi: https://doi.org/10.1101/333518; this version posted May 30, 2018. The copyright holder for this preprint (which was not certified by peer review) is the author/funder, who has granted bioRxiv a license to display the preprint in perpetuity. It is made available under aCC-BY 4.0 International license.

Dubois (1970b). The dimensions of the specimens we encountered also exceed values reported by Palmieri (1977), who reported means and standard deviations from adults from diverse hosts experimentally infected with metacercariae from centrarchids. However, as seen above, morphometric deviations relative to these studies were small, and Palmieri (1977) showed that adult morphology varies a great deal within *P. centrarchi*. Also, deviations were obtained from hologenophores genetically matching *P. centrarchi* common in centrarchid hosts (e.g., see records in (Boone et al., 2018; Locke et al., 2010)), and therefore there is no doubt they represent *P. centrarchi*.

The worm used in genomic analysis had partial CO1 sequences and ITS1-5.8S-ITS2 sequences 99-100% similar to those of *P. centrarchi* (=*Posthodiplostomum* sp. 3 of Locke et al., 2010; Stoyanov et al., 2017), including the hologenophore in Fig. 5, and CO1 from *P. centrarchi* from liver of *Lepomis microlophus* in Puerto Rico.

3.4.3 Cardiocephaloides medioconiger Dubois and Vigueras, 1949 (Fig. 6)

[Measurements from 3 hologenophores ex *Thallasius maximus*, Florida Keys, USA]

Total length 7273–8324; forebody and hindbody separated by moderate constriction. Forebody tulip-shaped 1333–1616 long, 1414–1455 wide. Hindbody 5657–6869 long, 1232–1293 wide, width gradually increasing posteriorly, widest at level of testes, tapering to point at posterior extremity. Hindbody 3.5–4.9 as long as forebody. Oral sucker 103–160 × 175–193. Ventral sucker 103–168 × 112–128. Tribocytic organ bi-lobed, with one lobe well developed and darkly staining. Pharynx 129–152 long, 119–152 wide. Ovary pretesticular, 363–363 long, 300–363 wide. Vitellaria dense in anterior hindbody, absent from ventral surface in region of ovary and testes, extending dorsally along anterior of copulatory bursa. Testicular zone 828–1010 long.

bioRxiv preprint doi: https://doi.org/10.1101/333518; this version posted May 30, 2018. The copyright holder for this preprint (which was not certified by peer review) is the author/funder, who has granted bioRxiv a license to display the preprint in perpetuity. It is made available under aCC-BY 4.0 International license.

Anterior testis 303–475 long, 606 wide. Posterior testis 363–484 long, 485–707 wide. Vitelline reservoir intertesticular. Eggs numerous 94–117 long, 62–70 wide with shells 2.0–2.2 thick. Copulatory bursa 1010–1919 long. Hindbody length 3.6–5.6 times that of copulatory bursa (means, standard deviations, n structures measured in Supplementary Table 3).

3.4.3.1 Remarks

Cardiocephaloides medioconiger was described from *Larus argentatus* in Cuba and has been reported from *T. maximus* in the same region (Dubois, 1970b). The morphology of the three voucher specimens was consistent with Dubois (1970b) (Supplementary Table 3), except that the following were larger: forebody (maxima of length and width of 1500 and 1360, respectively, in Dubois, 1970b), oral sucker (maximum width 136 in Dubois, 1970b) and ovary (maximum 278 × 300 in Dubois, 1970b). The four CO1 barcode sequences obtained were 99.1-99.8% similar to *C. medioconiger* (JX977783) from *Larus* sp. collected in Campeche, Mexico (Hernández-Mena et al., 2014). Within species of *Cardiocephaloides*, mean variation in CO1 is 0.7% (range 0-1.5%) and between species, 8.8% (range 7.4 -9.7%). The rDNA operon from the specimen we collected differed by 1.2% (1669/1672 identities) from 18S (MF398359, isolate DNA181) and 2.3% from the ITS (1041/1065 identities with JX977844, isolate DNA181) of *Cardiocephaloides* sp. from *Larus occidentalis* in Baja California, Mexico, and by 0.5% (1839/1848 identities) from 18S from *C. longicollis* (AY222089) from *Larus ridibundus*, Ukraine.

3.4.4.1 Cotylurus marcogliesei n. sp. (Fig. 7)

3.4.4.2 Description

[Measurements from 11 specimens (3 hologenophores, 7 paragenophores, and holotype), ex *Lophodytes cucullatus*]

bioRxiv preprint doi: https://doi.org/10.1101/333518; this version posted May 30, 2018. The copyright holder for this preprint (which was not certified by peer review) is the author/funder, who has granted bioRxiv a license to display the preprint in perpetuity. It is made available under aCC-BY 4.0 International license.

Adult total length 816–1152 (973±107, 10); forebody and hindbody separated by marked constriction. Body mildly arched dorsally. Forebody cup-shaped 216–408 (307±51, 11) long, 312–640 (436±95, 10) wide, with broad, oblique opening. Ventral forebody wall markedly shorter than dorsal. Hindbody stout along entire length, 600–880 (703±96, 10) long, 256–520 (318±81, 9) wide. Forebody to hindbody length ratio 1:1.9–2.8 (2.3±0.3, 10). Oral sucker terminal, 48–80 (68±13, 9) × 64–112 (85±15, 8). Ventral sucker 64–128 (99±24, 6) × 80–168 (108±28, 7). Tribocytic organ bilobed, with one or both lobes extending anteriorly beyond margin of forebody; proteolytic gland not observed. Pharynx small, difficult to observe, 28–34 (30±3, 3) long, 33–56 (43±12, 3) wide. Testes tandem, small, lobed and smooth; anterior testis 112–168 (132±27, 4) long, 112–120 (116±6, 2) wide, posterior margin at 32–45 (38±6, 4) % of hindbody. Posterior testis 136–160 (144±11, 4) long, 104–116 (110±8, 2) wide, with posterior margin at 59–67 (64±3, 5) % of hindbody. Ovary, near anterior extremity of hindbody, oval, 40–96 (68±40, 2) long, 56–56 (56±0, 2) wide. Vitellaria follicular, confined to hindbody, densely distributed in ventro-lateral field extending posteriorly to level of copulatory bursa and genital bulb, without obscuring the latter. Vitelline reservoir intertesticular; median. Uterus with 4–13 (9±3, 9) eggs, 76–108 (95±7.6, 37) long × 40–72 (56±6.9, 37) wide. Copulatory bursa large, genital bulb round, oval or reniform, 72–144 (111±27, 7) × 74–160 (117±27, 7).

3.4.4.3 Diagnosis

Adults of *Cotylurus marcogliesei* n. sp. possess a typically strigeid morphology, vitellaria confined to the hindbody, genital bulb in the copulatory bursa and smooth, bi- or trilobed testes with lobes pointing posteriorly, all of which are characteristic of *Cotylurus*. The wide opening of the forebody is more representative of *Ichthyocotylurus* Odening, 1969 (Niewiadomska, 2002b), but the presence of a genital bulb and testes with posterior facing lobes, in addition to CO1

bioRxiv preprint doi: https://doi.org/10.1101/333518; this version posted May 30, 2018. The copyright holder for this preprint (which was not certified by peer review) is the author/funder, who has granted bioRxiv a license to display the preprint in perpetuity. It is made available under aCC-BY 4.0 International license.

355 sequence similarity (Fig. 4) indicate the species belongs to *Cotylurus*. The most morphologically
356 similar species is *C. brevis* Dubois and Rausch, 1950, from which molecular data are
357 unavailable. The hindbody of *C. marcogliesei* n. sp. is 2.1–2.8 times as long as the forebody,
358 while in *C. brevis* it is 1.3–1.9 times as long (Dubois, 1970b) (Supplementary Table 4). Mature
359 adults of *C. marcogliesei* n. sp. are 816–1152 (mean 990) in total length, and half of the
360 specimens were shorter than the minimum length of *C. brevis* (1000–1800) (Dubois, 1970b). The
361 pharynx is shorter in *C. marcogliesei* n. sp. (28-34) than in *C. brevis* (50-59), although this organ
362 is difficult to visualize in both species (Dubois, 1970b) and may not be a reliable character for
363 identification or discrimination. To our knowledge, no members of the genus *Cotylurus* have
364 been recorded from *Lophodytes* (Anatidae, Merginae), which further distinguishes it from *C.*
365 *brevis*, originally described in Europe and found mainly in *Aythya* and *Anas* spp. (Anatidae,
366 Anatinae).

367 Type host*: Lophodytes cucullatus* (definitive host)

368 Site of infection*:* Small intestine (definitive host)

369 Type locality*:* Montreal, Quebec, Canada (50.183 N, –98.383 W) (definitive host)

370 Type material*:* Holotype (adult worm) Voucher accessions forthcoming;

371 Representative DNA sequences*:* CO1: XXXXXXX.

372 Etymology*:* The species is named after David J. Marcogliese, for his contributions to
373 parasitology.

374 Partial CO1 sequence was obtained from one of two specimens of *C. flabelliformis* from *Aythya*
375 *vallisneria* collected in Manitoba. The paragenophore was 782 long, with forebody 351 × 367,

bioRxiv preprint doi: https://doi.org/10.1101/333518; this version posted May 30, 2018. The copyright holder for this preprint (which was not certified by peer review) is the author/funder, who has granted bioRxiv a license to display the preprint in perpetuity. It is made available under aCC-BY 4.0 International license.

strongly arched dorsally, hindbody 638 × 399, oral sucker 64 × 96, pharynx 44 × 44, ventral sucker 88 × 112, eggs (n=30) 93-100 × 50-60, and its dimensions, morphology, host and geographic provenance agree with the collective accounts of Dubois (1970b), Campbell (1971) and Lapage (1961). Sequences of CO1 were obtained from three specimens of *Cotylurus strigeoides* Dubois, 1958 from *Aythya collaris*. The three hologenophores were 1818 long, with forebody 64 long, hindbody 1313-1475 ×747-768, oral sucker 160 × 112, pharynx 88 × 76, ventral sucker 192 × 136, ovary 152-231×128-207, anterior testis 223-283 × 239-423, posterior testis 271-319 × 271-343, eggs (39≤n≤79) 88-98 × 56-64. The CO1 sequences from *C. strigeoides* were 1.1-1.5% divergent from a CO1 sequence (JX977781) of a worm from *Aythya affinis* collected in Sonora, Mexico (Hernández-Mena et al., 2014). Because of the low level of divergence between *C. strigeoides* and JX977781, we believe all these data originate from *C. strigeoides*, but JX977781 is identified as *C. gallinulinae*. The material we examined was distinguished from *C. gallinulinae* by a large pharynx (5% of total length, and over half the size of the oral sucker, versus ≤2% of total length, and less than half the size of the oral sucker in *C. gallinulinae*, Dubois, 1970b), and the position of the ovary immediately posterior to the division of the fore- and hindbody (Dubois, 1958), whereas in *C. gallinulinae* it lies further posterior (Fig. 211 in Dubois (1970b). Records in Manitoba and Sonora are plausible for *C. strigeoides*, which is known from California and Alaska, whereas *C. gallinulinae* is neotropical (Dubois, 1970b; McDonald, 1981). Both JX977781 and the specimens we identified as *C. strigeoides* were from anatid hosts, which is typical for *C. strigeoides*, whereas *C. gallinulinae* is known from members of the Raillidae (Dubois, 1970b; McDonald, 1981). Within *Cotylurus* as whole, CO1 varies 0-0.3% (mean 0.2%) within species and 3.4-11.2% (mean 8.3%) between species (considering JX977781 as *C. strigeoides*). Sequences of CO1 from *C. marcogliesei* n. sp. differed by 7.9-

bioRxiv preprint doi: https://doi.org/10.1101/333518; this version posted May 30, 2018. The copyright holder for this preprint (which was not certified by peer review) is the author/funder, who has granted bioRxiv a license to display the preprint in perpetuity. It is made available under aCC-BY 4.0 International license.

399 9.3% from other species of *Cotylurus*. The rDNA operon of *C. marcogliesei* n. sp. differs from
400 other species of *Cotylurus* by 0.7-3% (JX977841, KY513180-2, MF398340).

401 *3.4.5 Alaria americana* Hall and Wigdor, 1918 (Fig. 8)

402 [Measurements from 8 specimens (2 hologenophores, 6 paragenophores), ex *Vulpes vulpes*,
403 Nova Scotia, Canada]

404 Total length 2121–2868; forebody and hindbody separated by shallow constriction. Forebody
405 with foliaceous lateral margins folded over ventral surface, 1375–1858 long, 465–869 wide.
406 Hindbody oval, 606–1010 long, 252–559 wide. Forebody 1.6–2.3 times longer than hindbody.
407 Lappets 136–240 long, with stippled glandular tissue along outer margin and protruding from
408 anterior extremity lateral to oral sucker, 64–120 × 50–119. Ventral sucker 88–104 × 88–120.
409 Tribocytic organ originating posterior to ventral sucker, 667–788 long, 160–250 wide. Pharynx
410 muscular, pyriform, 120–150 long, 45–96 wide, wider posteriorly, larger than oral sucker.
411 Pharynx length 1.2–2.0 times oral sucker length. Testes in anterior two thirds of hindbody.
412 Anterior testis smooth, unevenly lobed, lateral, 110–319 × 120–327, situated opposite Mehlis'
413 gland. Posterior testis sub-symmetrical, extending laterally across hindbody width, with two
414 lateral, round lobes, 80–223 × 152–270. Ovary lateral near anterior extremity of hindbody, round
415 to oval, 67–160 × 65–280 wide. Vitellaria mainly in forebody, dense in tribocytic organ,
416 extending anterior to or just past ventral sucker, extending posterior to or slightly beyond
417 forebody-hindbody constriction. Ejaculatory pouch fusiform, 250–444 × 101–135, with muscular
418 walls 31–55 thick, extending from posterior testis, or just posterior, to dorsally opening genital
419 atrium. Seminal vesicle with sinuous with transverse sections lying dorsal to ejaculatory pouch,
420 posterior to posterior testis. Vitelline reservoir intertesticular; median. Eggs 0–11, 102–136 long
421 × 36–80 wide. (means, standard deviations, n structures measured in Supplementary Table 5)

bioRxiv preprint doi: https://doi.org/10.1101/333518; this version posted May 30, 2018. The copyright holder for this preprint (which was not certified by peer review) is the author/funder, who has granted bioRxiv a license to display the preprint in perpetuity. It is made available under aCC-BY 4.0 International license.

422 *3.4.5.1 Remarks*

423 Dubois (1970b) considered *A. americana* a junior synonym of *A. marcianae*. The morphological,
424 molecular and life-history data herein support Johnson (1970) and Pearson and Johnson (1988),
425 who maintained *A. americana* as valid (Supplementary Table 5). Adults of *A. americana* are
426 larger (>2000) than those of *A. marcianae* (<2000) and have a thicker-walled ejaculatory pouch
427 (>20 compared with <20 in *A. marcianae*). The CO1 from adults from *Vulpes vulpes* in Nova
428 Scotia matched (i.e., 98.4-99.8% similarity) sequences from two mesocercariae from a
429 *Lithobates clamitans* in Quebec. Both *V. vulpes* and *L. clamitans* are known hosts of *A.*
430 *americana* in North America (Dubois, 1970b). Adults of this species occur in canid definitive
431 hosts, while *A. marcianae* mainly matures in felid and mustelid hosts (Pearson and Johnson,
432 1988). The adult *A. marcianae* sequenced in Uhrig et al. (2015) was collected from *Taxidea*
433 *taxus* (Mustelidae).

434 In *A. americana* and other *Alaria* spp., intraspecific CO1 distances range from 0 to 2.9% and
435 interspecific distances from 8.4 to 13.1% (total 53 CO1 sequences from *A. americana*, *A.*
436 *mustelae*, and *A. marcianae; A. marcianae* includes *Alaria* sp. 2 of Locke et al. (2011) as noted
437 by Uhrig et al. (2015), who recorded the sequence match but mistakenly referred to *Alaria* sp. 1
438 of Locke et al. (2011)). We also include here new CO1 records from *A. mustelae* from *Martes*
439 *pennanti* from Wisconsin.

440 The rDNA operon of *A. americana* assembled from genomic data differs by 2.2-13.5% from 13
441 sequences from *A. mustelae*, *A. marcianae*, *A. alata* and three unidentified species of *Alaria*
442 (comparisons of various regions of the rDNA array, limited to sequences overlapping > 500 bp,
443 AF184263, AY222091, JF769477-8, JF769480, JF769482, JF769484, JF820605, JF820607,
444 JF820609, KT254014, KT254021, KT254023). Notably, *A. americana* differs from *A.*

bioRxiv preprint doi: https://doi.org/10.1101/333518; this version posted May 30, 2018. The copyright holder for this preprint (which was not certified by peer review) is the author/funder, who has granted bioRxiv a license to display the preprint in perpetuity. It is made available under aCC-BY 4.0 International license.

445 *marcianae* by 6.1% in partial 28S rDNA (914/973 identities with KT254021-2, Uhrig et al.,
446 2015)) and by 8.4-8.9% in partial CO1 (KT254037-9, Uhrig et al. 2015).

447 *3.4.6 Hysteromorpha triloba* (Rudolphi, 1819) (Fig. 8, Supplementary Fig. 3)

448 [Metacercaria; measurements from 7 paragenophores, ex lateral and cheek muscle of *Squalius*
449 *cephalus* (mean weight 67 g) from Bidente River, Forlì-Cesena province, Emilia Romagna
450 region, Italy; 10/10 fish infected with hundreds of metacercariae.]

451 Total length 776–889 (830±42, 7); body oval or pyriform, with poor demarcation between
452 forebody and hindbody. Forebody round 536–664 (606±48, 7) long, 576–687 (630±33, 7) wide,
453 with pseudosuckers forming cup-shaped depressions 48–80 (64±12, 7) deep, 44–96 (69±14, 12)
454 wide. Hindbody bluntly triangular, roughly 120–303 (225±62, 7) long, 256–545 (404±96, 7)
455 wide at widest point, where it joins forebody. Oral sucker terminal, 72–125 (82±19, 7) long, 52–
456 84 (70±12, 7) wide. Pharynx 50–76 (61±10, 7) long, 30–44 (36±4, 7) wide. Ventral sucker 60–
457 82 (70±8, 7) long, 88–107 (99±6, 7) wide, sometimes anterior to, sometimes covered by
458 tribocytic organ. Tribocytic organ trilobed, 160–229 (193±27, 6) long, 163–320 (207±54, 7)
459 wide. Oesophagus 20–47 (34±19, 2) long, caeca almost reaching end of hindbody, flanking or
460 passing ventrally over genital primordia in hindbody.

461 *Hysteromorpha corti* comb. nov. (Hughes, 1929) (Fig. 10)

462 [Adult; measurements from 12 paragenophores, ex *Phalacrocorax auritus*, Montreal, Quebec,
463 Canada]

464 Total length 1052 – 1633 (1314±172, 12); forebody and hindbody separated by constriction.
465 Forebody spathulate, 490 - 762 (664±86, 12) long, 404 - 707 (509±82, 12) wide. Hindbody oval,
466 490 - 943 (658±125, 12) long, 381 - 636 (480±68, 12) wide. Pseudosuckers forming recessed

bioRxiv preprint doi: https://doi.org/10.1101/333518; this version posted May 30, 2018. The copyright holder for this preprint (which was not certified by peer review) is the author/funder, who has granted bioRxiv a license to display the preprint in perpetuity. It is made available under aCC-BY 4.0 International license.

467 depressions in forebody, 47 - 129 (78±26, 9) deep, 70 - 200 (105±38, 9) across. Oral sucker 50 -
468 107 (75±16, 12) × 71 - 107 (86±12, 12). Ventral sucker 36 - 107 (75±18, 11) × 43 - 143 (93±30,
469 11). Tribocytic organ 142 - 321 (241±58, 12) long, 190 - 293 (237±33, 11) wide. Pharynx
470 muscular, pyriform, 52–68 (59±6, 5) long, 40–70 (52±11, 5) wide. Ovary 71 - 100 (85±14, 5) ×
471 64 - 114 (81±19, 5), anterior to anterior testis. Anterior testis smooth, unevenly lobed, lateral,
472 107 - 214 (169±31, 10) × 107 - 250 (171±48, 7). Posterior testis extending laterally across
473 hindbody width, with two lateral, round lobes, 143 - 229 (171±35, 9) × 357 - 500 (423±51, 8).
474 Vitelline reservoir intertesticular; sub-median. Vitellaria from anterior to ventral sucker to
475 posterior extremity, forming a narrow ventral band in hindbody at level of testes. Genital atrium
476 subterminal, dorsal. Eggs 0–9, 87–109 (96±6, 12) long × 44–66 (54±6, 12) wide.

477 [Metacercaria; measurements from 7 syngenophores, ex *Catostomus commersoni* (n=1),
478 *Notemigonus crysoleucas* (n=5), Montreal and Great Lakes region, Canada]

479 Total length 712–880 (796±55, 7); body oval or shield-shaped, with poor demarcation between
480 forebody and hindbody. Forebody round 640–696 (670±25, 5) long, 384–472 (428±34, 7) wide.
481 Hindbody bluntly triangular, roughly 80–160 (126±32, 5) long, 152–200 (176±34, 2) wide at
482 widest point, where it joins forebody. Oral sucker terminal, 60–68 (62±4, 5) long, 56–68 (63±4,
483 5) wide. Pharynx 32–35 (33±2, 3) in diameter. Ventral sucker 56–68 (60±6, 5) long, 60–76
484 (73±6, 6) wide, sometimes anterior to, sometimes partly covered by tribocytic organ. Tribocytic
485 organ trilobed, 136–176 (163±18, 4) long, 116–160 (137±19, 5) wide.

486 *3.4.6.1 Diagnosis and Remarks*

487 Sequences of CO1 from metacercariae of *H. triloba* from Italy differed by 6.9-9.7 (mean 8.7)%
488 from material collected in North and Central America (Fig. 4). Among the Italian isolates, CO1

bioRxiv preprint doi: https://doi.org/10.1101/333518; this version posted May 30, 2018. The copyright holder for this preprint (which was not certified by peer review) is the author/funder, who has granted bioRxiv a license to display the preprint in perpetuity. It is made available under aCC-BY 4.0 International license.

489 varied by 0.3-0.8 (mean 0.5)%, and among American samples, by 0-5.6 (mean 1.7)%. The rDNA
490 operon of Italian *H. triloba* differed from American isolates by 0-0.2% from 18S and 28S
491 subunit sequences 1281-1694 bp in length (HM114365, MF398354-7) and by 0.1-0.3% to ITS1-
492 5.8S-ITS2 sequences 1017-1261 in length (HM064925-7, JF769486, MG649479-93). These 20
493 aligned ITS sequences from *Hysteromorpha* had three variable sites, with one transitional
494 mutation in ITS1 private to the Italian sequence. Rudolphi (1819) described *Hysteromorpha*
495 *triloba* (as *Distoma trilobum*) in Europe from four adults from *Phalacrocorax carbo* collected by
496 Bremser, who was based in Vienna (Sattmann et al., 2014). The type host has a wide, but mainly
497 Eurasian distribution (Hatch et al., 2000). A description of metacercaria of *H. triloba* from
498 cyprinids in Europe by Ciurea (1930) largely agrees with our observations of metacercariae from
499 *S. cephalus* (Cyprinidae), and the ventral and oral suckers, pharynx and oesophagus are generally
500 smaller in European than in American isolates (Supplementary Table 6). We consider these
501 European and American isolates of *Hysteromorpha* to be separate species, even if meristic or
502 morphological differences were not discerned between American and European adults of
503 *Hysteromoprha* based on available data and descriptions (Supplementary Table 6), and rDNA
504 divergence levels are small. Because the species was described in Europe, from a host with a
505 Palaearctic distribution, and similar metacercariae are known from cyprinids in Europe (see also
506 records in Bykhovskaya-Pavlovskaya, 1962), the name *H. triloba* is reserved for the Palearctic
507 lineage. In the Nearctic, Hughes (1929) provided the first description of *Hysteromorpha*, from
508 metacercariae in the muscle of *Ameiurus nebulosus* and *Ameiurus melas* in the Illinois River.
509 Hughes (1929) named these metacercariae *Diplostomulum corti*. Hugghins (1954a, 1954b)
510 synonymized *D. corti* with *Hysteromorpha triloba* (Rudolphi, 1819) Lutz 1931. The North
511 American species of *Hysteromorpha* will therefore bear the name created by Hughes (1929).

bioRxiv preprint doi: https://doi.org/10.1101/333518; this version posted May 30, 2018. The copyright holder for this preprint (which was not certified by peer review) is the author/funder, who has granted bioRxiv a license to display the preprint in perpetuity. It is made available under aCC-BY 4.0 International license.

512 *3.4.7 Tylodelphys immer* Dubois, 1961 (Fig. 11).

513 [Measurements from 5 adult paragenophores, ex *Gavia immer*.]

514 Total length 1515–1636; body linguiform, poor demarcation between forebody and hindbody.
515 Forebody 970–1111 long, 455–556 wide, oval in shape with pointed anterior flanked by
516 conspicuous pseudosuckers 160–232; forebody widest usually in anterior third (4/5 specimens).
517 Ventral surface tegument with plicate folds on anterior half to two thirds of forebody. Cylindrical
518 hindbody tapering to terminate in rounded extremity, 525–566 long, 284–404 wide. Hindbody
519 length / forebody length 0.47–0.56; hindbody width / forebody width 0.51–0.85. Oral sucker
520 terminal, 80–119 long, 100–127 wide. Pharynx well developed, 68–84 long, 66–80 wide. Ventral
521 sucker 90–109 long, 100–131 wide, situated slightly more than halfway along length of
522 forebody, the anterior edge occurring 51–54% from anterior end of forebody. Tribocytic organ
523 oval to round, 240–288 long, 152–240 wide. Ovary round or bilobed, small, sub-median, near or
524 overlapped by postero-lateral edge of tribocytic organ, 40–80 long, 56–80 wide. Testicular zone
525 extending posteriorly from forebody-hindbody division, occupying first 29–39% of hindbody.
526 Testes tandem, symmetric, bilobed. Anterior testis 80–96 long, 272–344 wide, wider than
527 posterior testis. Posterior testis 88–112 long, 272–320 wide. Vitelline field densest in vicinity of
528 tribocytic organ, extending two thirds of length of forebody, ending 31–34% of distance from
529 anterior edge of ventral sucker to anterior extremity, in hindbody narrowing to a ventral strip
530 between lobes of posterior testis, terminating in a lateral band at level of seminal vesicle.
531 Vitelline reservoir intertesticular, sub-median. Copulatory bursa with subterminal, wide, thick-
532 walled ventral opening 168–184 long, 160–184 wide, housing well-developed genital cone 112–
533 152 wide. Uterus with 1–8 eggs, 82–100 long × 44–68 wide.

534 *3.4.8 Remarks*

bioRxiv preprint doi: https://doi.org/10.1101/333518; this version posted May 30, 2018. The copyright holder for this preprint (which was not certified by peer review) is the author/funder, who has granted bioRxiv a license to display the preprint in perpetuity. It is made available under aCC-BY 4.0 International license.

Most of these observations and dimensions agree with the account of Dubois (1970b) (supplementary Table 7), although he did not comment on the tegument; a pseudosucker on one specimen was shorter (160 *versus* 180 minimum length in Dubois, 1970b); the pharynx was wider in three worms (74-80 *versus* maximum of 70 in Dubois, 1970b); the ventral sucker was longer in 4 worms (104–109 *versus* 100 in Dubois (1970b) and wider in one (131 *versus* 122 in Dubois, 1970b); the ovary was smaller (40–80×56–80 *versus* 95–115×80–145 in Dubois, 1970b) and more median in 3 worms; the anterior testis was shorter in 3 worms (80-88 versus 90 in Dubois, 1970b), the posterior in one (88 versus 90 in Dubois, 1970b); and the genital cone was wider in 2 worms (152 *versus* 135 in Dubois, 1970b). These variations seem within that to be expected within species, and thus not taxonomically significant. They could reflect differences in maturity, as the worms included in our analysis had 0-8 eggs, while Dubois (1970b) examined material with 4-17 eggs, or again might be artefacts of differences in specimen preparation.

The specimens used for morphological and genomic analysis in the present study were from the same individual host as the *T. immer* studied by Locke et al. (2015), and the mitochondrial genome and rDNA operon were 98.1-99.9 % similar to CO1 (Fig. 4) and identical to ITS sequences (KT186804-6) of Locke et al. (2015).

4. Discussion

We confirmed and expanded on recent analyses showing a paraphyletic pattern of mt genome evolution in the Diplostomida (Brabec et al., 2015; Briscoe et al., 2016; Chen et al., 2016). The mt genomic phylogeny conflicts with the rDNA phylogeny upon which the Diplostomida was erected (Figs. 1, 2). There were about one quarter as many variable sites in the rDNA alignment as in our alignment of mt nucleotides (1444 variable sites in Olson et al., 2003). Thus, the well-supported mt topology in Fig. 2, containing members of two of three

bioRxiv preprint doi: https://doi.org/10.1101/333518; this version posted May 30, 2018. The copyright holder for this preprint (which was not certified by peer review) is the author/funder, who has granted bioRxiv a license to display the preprint in perpetuity. It is made available under aCC-BY 4.0 International license.

558 superfamilies in the Diplostomida, might have cast doubt on the validity of the order. However, a
559 much larger genomic dataset, which we had designated as an arbiter between mitonuclear
560 alternatives, yielded unequivocal support for the order (Fig. 3).

561 Discordance between nuclear and mt phylogenies is not uncommon, and although it is
562 more often recorded at shallower nodes than in the present study (e.g., Perea et al., 2016; Platt et
563 al., 2018), differences also occur among deeply divergent lineages (e.g., Sun et al., 2015, and
564 compare Inoue et al., 2003 and Faircloth et al., 2013). In the present case, the discrepancy occurs
565 along short internal branches at the base of longer terminal branches (Figs. 2, 3). This is
566 consistent with ancient, rapid radiation, which is inherently difficult to resolve, particularly in
567 conjunction with incomplete lineage sorting (Whitfield and Lockhart, 2007). Along these short
568 internal branches, mitochondrial genomes of digeneans may have a lower phylogenetic
569 signal/noise ratio than nuclear genes, exacerbating effects of incomplete taxon sampling
570 (Graybeal and Cannatella, 1998; Hedtke et al., 2006; Philippe et al., 2011). Genomic data (both
571 mt and nuclear) from other diplostomidans and early, divergent lineages from the Plagiorchiida
572 are needed to clarify this (Brachylaimoidea Joyeux and Foley, 1930, Liolopidae Odhner, 1912,
573 Aporocotylidae Odhner, 1912, Spirorchiidae Stunkard, 1921, Bivesiculoidea Yamaguti, 1934).

574 Within the Diplostomoidea, however, the mt and UCE phylogenies are congruent, which
575 suggests they reflect evolutionary relationships among the species studied. Figures 2 and 3 also
576 share elements that recur in prior work. In most molecular phylogenies, the superfamily is
577 monophyletic and cyathocotylids are basal (Blasco-Costa and Locke, 2017; Dzikowski et al.
578 2004; Hernández-Mena et al., 2017), as herein. Both the branching order and composition of the
579 major diplostomoid clades in Figs. 2 and 3 herein are consistent with an analysis of concatenated
580 CO1 and rDNA spacer sequences by Blasco-Costa and Locke (2017). The association of

bioRxiv preprint doi: https://doi.org/10.1101/333518; this version posted May 30, 2018. The copyright holder for this preprint (which was not certified by peer review) is the author/funder, who has granted bioRxiv a license to display the preprint in perpetuity. It is made available under aCC-BY 4.0 International license.

581 *Hysteromorpha*, *Alaria, Tylodelphys* and *Diplostomum* is consistent with trees in Fraija-
582 Fernández et al. (2015), López-Jiménez et al. (2017), and Olson et al. (2003). Discrepancies
583 (e.g., *Hysteromorpha* in Hernández-Mena et al., 2017) are typically associated with poor nodal
584 support. These genera are also consistently associated with *Austrodiplostomum* and
585 *Neodiplostomum* (Blasco-Costa and Locke, 2017; Hernández-Mena et al., 2017; Locke et al.,
586 2015; the latter sometimes misidentified as *Fibricola*, see Blasco-Costa and Locke, 2017), and
587 the name Diplostomidae should be reserved for members of this group.

588 Like other studies, our analysis indicates the Diplostomidae *s.l.* is paraphyletic.
589 *Posthodiplostomum*, though nominally part of the family, is separate from and basal to a clade
590 composed of other diplostomids and the Strigeidae. *Posthodiplostomum* belongs to the
591 Crassiphialinae Sudarikov, 1960 and is consistently recovered with other members of this
592 subfamily (e.g., *Uvulifer, Bolbophorus*, *Ornithodiplostomum*, *Mesoophorodiplostomum* and
593 *Posthodiplostomum* in Athokpam and Tandon, 2014; Blasco-Costa and Locke, 2017; Hernández-
594 Mena et al., 2017; López-Jiménez et al., 2017; Sereno-Uribe et al., 2018; Locke et al., 2010, see
595 fig. S4). One recent analysis suggests some of these genera are not distinct (López-Hernández et
596 al., 2018). As noted by Blasco-Costa and Locke (2017) and Hernández-Mena et al. (2017), it
597 appears that the Crassiphialinae will rise to the family level, although it would be prudent to
598 obtain data from the type genus, *Crassiphiala* Van Haitsma, 1925, before enacting this.

599 Both the present and the weight of prior phylogenetic analysis (see above) suggest that
600 some family-level clades in the Diplostomoidea are distinguishable by long-recognized
601 metacercarial morphotypes. For example, crassiphialinids and other diplostomids are clearly
602 evolutionarily distinct, and readily separated by their metacercariae (neascus and
603 diplostomulum). In adult forms, members of these two clades are sometimes discriminated by

bioRxiv preprint doi: https://doi.org/10.1101/333518; this version posted May 30, 2018. The copyright holder for this preprint (which was not certified by peer review) is the author/funder, who has granted bioRxiv a license to display the preprint in perpetuity. It is made available under aCC-BY 4.0 International license.

604 the distribution of the vitellaria, but this character fails in many cases (Niewiadomska, 2002c).
605 The view that the metacercaria offers an impoverished subset of the phylogenetically informative
606 characters found in the adult (Gibson, 1987) seems not to apply in the Diplostomoidea. For
607 example, the infection sites and encystment habits of metacercariae may be phylogenetically
608 conserved. Diplostomid genera with metacercariae that reside unencysted in the eyes of second
609 intermediate hosts consistently group together in molecular phylogenies (Blasco-Costa and
610 Locke, 2017; Hernández-Mena et al., 2017) and in *Diplostomum*, habitats within the eye are
611 conserved (Blasco-Costa et al., 2014) and may influence diversification (Locke et al., 2015).
612 Some morphological characters are also more easily visualized in metacercariae. For example,
613 the character that mapped best onto phylogenetic analysis herein, the structure of the reserve
614 bladder, is seldom described in the adult, likely because it is obscured by reproductive structures
615 in mature worms (for an exception, see Overstreet et al., 2002). The value of this character fits
616 Niewiadomska's (2002a) concept of four main morphotypes. Shoop (1989) distinguished
617 additional types of metacercariae, but molecular phylogenies have not supported their
618 distinctness (e.g., see *Neodiplostomum/Fibricola*, and *Bolbophorus*, which possess neo- and
619 prodiplostomula in Shoop's system, in Blasco-Costa and Locke, 2017; Hernández-Mena et al.,
620 2017). Further assessing the evolution of metacercarial characters and morphotypes will require
621 additional molecular and morphological analysis. In the Strigeidae, all metacercariae are of a
622 single type (tetracotyle), but the family is frequently non-monophyletic in molecular studies
623 (Blasco-Costa and Locke, 2017; Hernández-Mena et al., 2017). It would be fruitful to
624 characterize the reserve bladder in metacercariae belonging to the Proterodiplostomidae, which
625 Hernández-Mena et al. (2017) found to be an early diverging, but not basal member of the
626 diplostomoid clade. The simpler reserve bladder in the Cyathocotylidae, and the reticulate forms

bioRxiv preprint doi: https://doi.org/10.1101/333518; this version posted May 30, 2018. The copyright holder for this preprint (which was not certified by peer review) is the author/funder, who has granted bioRxiv a license to display the preprint in perpetuity. It is made available under aCC-BY 4.0 International license.

627 with transverse commisures in the crown clade of Strigeidae and Diplostomidae, predict
628 intermediate complexity in proterodiplostomids.

629 The initial aim of this study was a phylogenomic evaluation of higher relationships
630 among a small number of worms. To this end, we selected seven specimens identified to genus
631 that were promising for shotgun sequencing. After closer examination of vouchers, we recorded
632 a new species of *Cotylurus*, resurrected a species of *Hysteromorpha*, and found support for a
633 species of *Alaria* of contested validity, and these findings were supported with molecular data.
634 Identifications were less than straightforward in 3/7 cases, a proportion similar to the 20/44
635 studies in which diplostomoid diversity differed from expectations (reviewed by Blasco-Costa
636 and Locke, 2017). One taxonomic result involved reconsideration of *H. triloba*, which has long
637 been thought to be cosmopolitan (Hugghins, 1954b; Locke et al., 2011; Lutz, 1931; Sereno-
638 Uribe et al., 2018). The genetic divergence seen in *Hysteromorpha* could be construed as
639 intraspecific variation in widely separated populations (particularly the low level of rDNA
640 variation), but we believe recently formed species to be a more plausible explanation. In addition
641 to the molecular evidence, the non-overlapping ranges of the definitive hosts of Nearctic and
642 Paleartic *Hysteromorpha* (i.e., *Phalacrocorax* spp.) suggest long isolation, and the distinction
643 between *H. triloba* and *H. corti* are supported by morphological differences in the metacercaria.
644 Moreover, the finding that *Hysteromorpha* is represented by a distinct species in North America,
645 *H. corti*, is consistent with a general trend. With sequences now available from thousands of
646 specimens and many valid and putative species of diplostomoids and clinostomids,
647 intercontinental distributions supported by molecular data are exceedingly rare, and limited to
648 distributions along the margins of a second continent (e.g., *Austrodiplostomum compactum* (=*A.*
649 *ostrowskiae*), Locke et al. 2015). More commonly, a single species thought to cosmopolitan is

bioRxiv preprint doi: https://doi.org/10.1101/333518; this version posted May 30, 2018. The copyright holder for this preprint (which was not certified by peer review) is the author/funder, who has granted bioRxiv a license to display the preprint in perpetuity. It is made available under aCC-BY 4.0 International license.

revealed by DNA to be comprised of multiple geographically isolated species (e.g., *Diplostomum spathaceum*, *D. baeri*, *Clinostomum complanatum*, Caffara et al., 2011; Galazzo et al., 2002; Locke et al., 2015). The presence of the North American species, *P. centrarchi*, in Europe (Kvach et al., 2017; Stoyanov et al., 2017) and the Caribbean (Bunkley-Williams and Williams, 1994; present study) is instructive, as it is associated with recent introductions of non-native intermediate hosts. The overall pattern suggests intercontinental distributions based on historical records should be regarded skeptically in diplostomoids, clinostomids, and, we would suggest, other digeneans with life cycles tied to fresh water. For example, we predict that DNA will reveal that Palearctic *Apharyngostrigea cornu* is distinct from North American isolates sequenced by Locke et al. (2011). Because *A. cornu* was described in Europe (Zeder, 1800), the North American lineage will need to be renamed. Similarly, the Holarctic distribution of *Cotylurus brevis* (Dubois, 1970b; McDonald, 1981) seems doubtful. South American isolates of *H. triloba* (Lunaschi et al., 2007; Lutz, 1931) are also likely to represent another species, distinct from the North American and European lineages.

Acknowledgements

We are indebted to Brandon Ballengée (McGill University), Kimberly Bates (Winona State University), Matías J. Cafaro (University of Puerto Rico at Mayagüez, UPRM), Gary Conboy (University of Prince Edward Island), Martin Kalbe (Max Planck Institute for Evolutionary Biology), David Kerstetter (Nova Southeastern University), Audrey J. Majeske (UPRM), J. Daniel McLaughlin (Concordia University), and Le Nichoir Wildlife Rehabilitation Centre for providing hosts, worms, or laboratory access. Lutz Froenicke and staff at the UC Davis Genome Center are gratefully acknowledged. Isabel Blasco-Costa (Natural History Museum of Geneva) provided constructive suggestions that improved an earlier version of the manuscript. Early

bioRxiv preprint doi: https://doi.org/10.1101/333518; this version posted May 30, 2018. The copyright holder for this preprint (which was not certified by peer review) is the author/funder, who has granted bioRxiv a license to display the preprint in perpetuity. It is made available under aCC-BY 4.0 International license.

673 phases of this study were supported by the Canadian Federal Government's Genomics Research
674 Development Initiative, an NSERC Discovery Grant (A6979), and by Paul D. N. Hebert at the
675 Center for Biodiversity Genomics, University of Guelph, Canada through funding from NSERC,
676 Genome Canada, the Ontario Genomics Institute and the International Barcode of Life initiative.
677 Major funding support was provided by the Puerto Rico Science, Technology and Research Trust
678 to SL and computational support was provided to by an NSF-XSEDE grant (TG-BIO170048) SL
679 and AVD.

680 **Figure legends**

681 **Fig. 1**. Schematic of phylogenetic conflict in the Digenea emerging from prior studies. Analysis
682 of nuclear rDNA (nDNA) indicates *Diplostomum*, *Clinostomum*, and *Schistosoma* belong to the
683 Diplostomida (Olson et al., 2003), while mitochondrial genomes (mtDNA) indicate
684 *Diplostomum* and *Clinostomum* belong to the Plagiorchiida (Brabec et al., 2015; Briscoe et al.,
685 2016; Chen et al., 2016). A polytomy occurs in the mitochondrial phylogeny because
686 *Diplostomum* and *Clinostomum* have not been included together in prior analysis.

687 **Fig. 2**. Phylogenetic analysis of seven representatives of the Diplostomoidea and 29 other
688 members of the Platyhelminthes, estimated using maximum likelihood based on 5647 variable
689 sites in 13 protein-coding genes in the mitochondrion. Nodes are labelled with support from
690 1000 bootstrap replicates, with support from analysis of translated amino acids (supplementary
691 Fig. 2) after the slash. Unlabelled nodes indicate support of 100/100. An asterisk and grey branch
692 indicate topological inconsistency with analysis of amino acids. GenBank accessions of
693 sequences from other studies are AF215860.1, AF216697.1, AF217449.1, AF219379.2,
694 DQ157222.2, DQ157223.1, DQ859919.1, DQ985706.1, EU921260.2, FJ381664.2, HE601612.1,
695 KC330755.1, KF214770.1, KF318786.1, KF318787.1, KF475773.1, KF543342.1, KM280646.1,

bioRxiv preprint doi: https://doi.org/10.1101/333518; this version posted May 30, 2018. The copyright holder for this preprint (which was not certified by peer review) is the author/funder, who has granted bioRxiv a license to display the preprint in perpetuity. It is made available under aCC-BY 4.0 International license.

696 KM923964.1, KP844722.1, KR269763.1, KR269764.1, KR703278.1, KT239342.1,
697 KU060148.1, KU641017.1, KX169163.1, KX765277.1, MF136777.1.

698 **Fig. 3**. Maximum likelihood analysis of 517 conserved genetic elements from seven members of
699 the Diplostomoidea, and other Platyhelminthes. The gray or black shaded boxes indicate families
700 recognized by Dubois (Dubois, 1938, 1970b) and Niewiadomska (Niewiadomska, 2002a).
701 Colors in matrix at right encode morphological and life history characters separated by
702 developmental stage (supplementary Table 1). Metacercarial morphotypes indicated at far right
703 are: P=prohemistomulum, D=diplostomulum, N=neascus, T=tetracotyle. The alignment is
704 234,783 bp in length, with 149,881 (64%) invariant and 84,902 (36%) variable sites. The
705 analysis was based on 90% matrix occupancy. Nodes had 100% support in 1000 bootstrap
706 replicates, except where indicated. Accessions of non-diplostomoid genomes obtained from
707 Wormbase (Howe et al., 2016) are PRJEB1206, PRJDA72781, PRJEB6687, PRJEB1207.

708 **Fig. 4**. Neighbour-joining tree of uncorrected p-distance among 195 partial sequences of
709 cytochrome *c* oxidase I (CO1). Shaded clades had >99% support in 500 bootstrap replicates in
710 ML analysis (not shown) and are annotated with identifications, host and geographic records
711 mentioned in the results. Sequences from the present study were obtained from species labelled
712 in bold. This includes Sanger-sequenced amplicons of the barcode region of COI (n=35,
713 XXXXXX-X) and mitochondrial genomes of specimens used in Figures 2 and 3. Sequences
714 (n=160) from other studies are FJ477182, FJ477203, FJ477217, HM064651-9, HM064712,
715 HM064714-7, HM064799-843, JF769422-76, JF904528-36, JX977781-4, KR271481-93,
716 KT254037-9, KX931421-3, KY513231-6, MF124272-3, MF398316, MG649464-78.

bioRxiv preprint doi: https://doi.org/10.1101/333518; this version posted May 30, 2018. The copyright holder for this preprint (which was not certified by peer review) is the author/funder, who has granted bioRxiv a license to display the preprint in perpetuity. It is made available under aCC-BY 4.0 International license.

717 **Fig. 5.** Adult of *Posthodiplostomum centrarchi* Hoffman, 1958, from *Ardea herodias*, Ile aux
718 Herons, St. Lawrence River, Quebec, Canada. Scale = 200 µm. Hologenophore for partial
719 sequence of cytochrome *c* oxidase I, Genbank accession XZXXXXXX.

720 **Fig. 6.** Adult of *Cardiocephaloides medioconiger* Hall & Wigdor, 1918, from *Thalassius*
721 *maximus*, Florida, United States. Scale = 2000 µm. Hologenophore for partial sequence of
722 cytochrome *c* oxidase I, Genbank accession XZXXXXXX.

723 **Fig. 7.** Adults of *Cotylurus marcogliesei* n. sp. from *Lophodytes cucullatus* in Montreal, Quebec,
724 Canada. Scale = 200 µm. Hologenophores for Genbank accession XZXXXXX.

725 **Fig. 8.** Adult of *Alaria americana* Hall & Wigdor, 1918, from *Vulpes vulpes*, Nova Scotia,
726 Canada. Scale = 500 µm. Paragenophore for partial sequence of cytochrome *c* oxidase I,
727 Genbank accession XZXXXXXX.

728 **Fig. 9.** Metacercariae of *Hysteromorpha triloba* (Rudolphi, 1819) from *Squalius cephalus*, Italy.
729 Scale = 200 µm. Paragenophores for partial sequence of cytochrome *c* oxidase I, Genbank
730 accession XZXXXXXX.

731 **Fig. 10.** Adult of *Hysteromorpha corti* (Hughes, 1929) from *Phalacrocorax auritus*, Montreal,
732 Quebec, Canada. Italy. Scale = 200 µm. Paragenophore for partial sequence of cytochrome *c*
733 oxidase I, Genbank accession XZXXXXXX.

734 **Fig. 11 (a).** Adult of *Tylodelphys immer* Dubois, 1961, from *Gavia immer* in Montreal, Quebec,
735 Canada. Scale = 200 µm. (**b).** Ventral tegument of forebody. VS=ventral sucker, arrow points to
736 anterior of worm. Scale = 50 µm. Paragenophore for partial sequence of cytochrome *c* oxidase I,
737 Genbank accessions KR271483, KR271487, KR271489.

bioRxiv preprint doi: https://doi.org/10.1101/333518; this version posted May 30, 2018. The copyright holder for this preprint (which was not certified by peer review) is the author/funder, who has granted bioRxiv a license to display the preprint in perpetuity. It is made available under aCC-BY 4.0 International license.

738 **Supplementary Fig. 1.** Characters mapped onto the topology of the phylogenomic analysis of
739 the Diplostomoidea.

740 **Supplementary Fig. 2**. Phylogenetic analysis of seven representatives of the Diplostomoidea
741 and 29 other members of the Platyhelminthes, estimated using maximum likelihood based on
742 translated amino acids in 13 protein-coding genes in the mitochondrion

743 **Supplementary Fig. 3**. Metacercaraie of *Hysteromorpha triloba* in muscle of *Squalius cephalus*.
744 A-B: live metacercariae (scale = 100 μm); Metacercariae in cheek (C), lateral (D) and caudal (E)
745 muscle.

746 **Supplementary Table 1.** Characteristics of mitochondrial genomes and rDNA operons for seven
747 members of the Diplostomoidea.

748 **Supplementary Table 2.** Selected morphometrics from adults of *Posthodiplostomum* reported in
749 μm as range (mean, ± standard deviation, n).

750 **Supplementary Table 3**. Selected morphometrics from adults of *Cardiocephaloides*
751 *medioconiger* reported in μm as range (mean, ± standard deviation, n).

752 **Supplementary Table 4.** Selected morphometrics from adults of *Cotylurus* reported in μm as
753 range (mean, ± standard deviation, n).

754 **Supplementary Table 5**. Selected morphometrics from adults of *Alaria* reported in μm as range
755 (mean, ± standard deviation, n).
756

bioRxiv preprint doi: https://doi.org/10.1101/333518; this version posted May 30, 2018. The copyright holder for this preprint (which was not certified by peer review) is the author/funder, who has granted bioRxiv a license to display the preprint in perpetuity. It is made available under aCC-BY 4.0 International license.

Supplementary Table 6. Selected morphometrics from metacercariae and adults of *Hysteromorpha* from the present and other studies, reported in µm as range (mean, ± standard deviation, n).

Supplementary Table 7. Selected morphometrics from adults of *Tylodelphys immer* reported in µm as range (mean, ± standard deviation, n).

References

Athokpam, V., Tandon, V., 2014. Morphological and molecular characterization of *Posthodiplostomum* sp. (Digenea: Diplostomidae) metacercaria in the muscles of snakeheads (*Channa punctata*) from Manipur, India. Helminthologia 51, 141–152.

Bernt, M., Donath, A., Jühling, F., Externbrink, F., Florentz, C., Fritzsch, G., Pütz, J., Middendorf, M., Stadler, P.F., 2013. MITOS: improved de novo metazoan mitochondrial genome annotation. Mol. Phylogenet. Evol. 69, 313–319.

Blasco-Costa, I., Faltýnková, A., Georgieva, S., Skírnisson, K., Scholz, T. and Kostadinova, A., 2014. Fish pathogens near the Arctic Circle: molecular, morphological and ecological evidence for unexpected diversity of *Diplostomum* (Digenea: Diplostomidae) in Iceland. Int. J. Parasitol. 44, 703–715.

Blasco-Costa, I., Locke, S.A., 2017. Life history, systematics and evolution of the Diplostomoidea Poirier, 1886: progress, promises and challenges emerging from molecular studies. Adv. Parasitol. 98, 167-244.

Blasco-Costa, I., Poulin, R., Presswell, B., 2016. Morphological description and molecular analyses of *Tylodelphys* sp. (Trematoda: Diplostomidae) newly recorded from the freshwater fish *Gobiomorphus cotidianus* (common bully) in New Zealand. J. Helminthol. 91, 332-345

Blasco-Costa, Isabel, Poulin, R., Presswell, B., 2016. Species of *Apatemon* Szidat, 1928 and *Australapatemon* Sudarikov, 1959 (Trematoda: Strigeidae) from New Zealand: linking and characterising life cycle stages with morphology and molecules. Parasitol. Res. 115, 271–289.

Boone, E.C., Laursen, J.R., Colombo, R.E., Meiners, S.J., Romani, M.F., Keeney, D.B., 2018. Infection patterns and molecular data reveal host and tissue specificity of *Posthodiplostomum* species in centrarchid hosts. Parasitology (In press) DOI: 10.1017/S0031182018000306

Brabec, J., Kostadinova, A., Scholz, T., Littlewood, D.T.J., 2015. Complete mitochondrial genomes and nuclear ribosomal RNA operons of two species of *Diplostomum* (Platyhelminthes: Trematoda): a molecular resource for taxonomy and molecular epidemiology of important fish pathogens. Parasit. Vectors 8, 1–11.

Briscoe, A.G., Bray, R.A., Brabec, J., Littlewood, D.T.J., 2016. The mitochondrial genome and ribosomal operon of *Brachycladium goliath* (Digenea: Brachycladiidae) recovered from a stranded minke whale. Parasitol. Int. 65, 271–275.

bioRxiv preprint doi: https://doi.org/10.1101/333518; this version posted May 30, 2018. The copyright holder for this preprint (which was not certified by peer review) is the author/funder, who has granted bioRxiv a license to display the preprint in perpetuity. It is made available under aCC-BY 4.0 International license.

797 Brooks, D.R., O'Grady, R.T., Glen, D.R., 1985. Phylogenetic analysis of the Digenea
798 (Platyhelminthes: Cercomeria) with comments on their adaptive radiation. Can. J. Zool.
799 63, 411–443.
800 Bunkley-Williams, L., Williams, E.H., 1994. Parasites of Puerto Rican freshwater sport fishes.
801 Department of Natural and Environmental Resources, San Juan, PR.
802 Bushnell, B., 2014. BBMap: A Fast, Accurate, Splice-Aware Aligner. Presented at the 9th
803 Annual Genomics of Energy & Environment Meeting, USDOE Office of Science (SC),
804 Walnut Creek, CA.
805 Bykhovskaya-Pavlovskaya, I.E., 1962. Key to Parasites of Freshwater Fish of the U.S.S.R., Keys
806 to Fauna of the U.S.S.R. Izdatelstvo Akademii Nauk SSSR.
807 Caffara, M., Locke, S.A., Gustinelli, A., Marcogliese, D.J., Fioravanti, M.L., 2011.
808 Morphological and molecular differentiation of *Clinostomum complanatum* and
809 *Clinostomum marginatum* (Digenea: Clinostomidae) metacercariae and adults. J.
810 Parasitol. 97, 884–891.
811 Campbell, R., 1971. Biology and development of *Cotylurus flabelliformis* (Trematoda:
812 Strigeidae). PhD Thesis. Iowa State University, Ames, Iowa.
813 Chaudhary, A., Gupta, S., Verma, C., Tripathi, R., Singh, H.S., 2017. Morphological and
814 molecular characterization of metacercaria of *Tylodelphys* (Digenea: Diplostomidae)
815 from the piscine host, *Mystus tengara* from India. J. Parasitol. 103, 565–573.
816 Chen, L., Feng, Y., Chen, H.-M., Wang, L.-X., Feng, H.-L., Yang, X., Mughal, M.-N., Fang, R.,
817 2016. Complete mitochondrial genome analysis of *Clinostomum complanatum* and its
818 comparison with selected digeneans. Parasitol. Res. 115, 3249–3256.
819 Chibwana, F.D., Blasco-Costa, I., Georgieva, S. Hosead, K.M., Nkwengulila, G., Scholz, T.,
820 Kostadinova, A. 2013. A first insight into the barcodes for African diplostomids
821 (Digenea: Diplostomidae): Brain parasites in *Clarias gariepinus* (Siluriformes:
822 Clariidae). Infection, Genetics and Evolution. 17, 62-70.
823 Ciurea, I., 1930. Contributions à l'étude morphologique et biologique de quelques strigeidés des
824 oiseaux ichtyophages de la faune de Roumanie (recherches expérimentales). Arch. Roum.
825 Pathol. Expérimentale Microbiol. 3, 277–323.
826 Cort, W.W., 1917. Homologies of the excretory system of the forked-tailed cercariae: A
827 preliminary report. J. Parasitol. 4, 49.
828 Dubois, G., 1970a. Les fondements de la taxonomie des Strigeata La Rue (Trematoda: Strigeida).
829 Rev. Suisse Zool. 77.
830 Dubois, G., 1970b. Synopsis des Strigeidae et des Diplostomatidae (Trematoda). Mém. Société
831 Neuchâtel. Sci. Nat. 10, 1–727.
832 Dubois, G., 1958. Les Strigeida (Trematoda) de Californie de la collection June Mahon. Bull.
833 Société Neuchâtel. Sci. Nat. 81, 69–78.
834 Dubois, G., 1938. Monographie des Strigeida (Trematoda). Mém. Société Neuchâtel. Sci. Nat. 6,
835 1–535.
836 Dzikowski, R., Levy, M.G., Poore, M.F., Flowers, J.R., Paperna, I., 2004. Use of rDNA
837 polymorphism for identification of Heterophyidae infecting freshwater fishes. Dis. Aquat.
838 Organ. 59, 35–41.
839 Faircloth, B.C., 2016. PHYLUCE is a software package for the analysis of conserved genomic
840 loci. Bioinformatics 32, 786–788.

bioRxiv preprint doi: https://doi.org/10.1101/333518; this version posted May 30, 2018. The copyright holder for this preprint (which was not certified by peer review) is the author/funder, who has granted bioRxiv a license to display the preprint in perpetuity. It is made available under aCC-BY 4.0 International license.

841 Faircloth, B.C., Sorenson, L., Santini, F., Alfaro, M.E., 2013. A phylogenomic perspective on the
842 radiation of ray-finned fishes based upon targeted sequencing of Ultraconserved
843 Elements (UCEs). PLoS ONE 8, e65923.
844 Fraija-Fernández, N., Olson, P.D., Crespo, E.A., Raga, J.A., Aznar, F.J., Fernández, M., 2015.
845 Independent host switching events by digenean parasites of cetaceans inferred from
846 ribosomal DNA. Int. J. Parasitol. 45, 167–173.
847 Galazzo, D.E., Dayanandan, S., Marcogliese, D.J., McLaughlin, J.D., 2002. Molecular
848 systematics of some North American species of *Diplostomum* (Digenea) based on rDNA-
849 sequence data and comparisons with European congeners. Can. J. Zool. 80, 2207–2217.
850 Gibson, D.I., 1996. Guide to the Parasites of Fishes of Canada: Trematoda, Canadian Special
851 Publication of Fisheries and Aquatic Sciences. NRC Research Press.
852 Gibson, D.I., 1987. Questions in digenean systematics and evolution. Parasitology 95, 429-460.
853 Gibson, D.I., Bray, R.A., 1994. The evolutionary expansion and host-parasite relationships of the
854 Digenea. Int. J. Parasitol. 24, 1213–1226.
855 Graybeal, A., Cannatella, D., 1998. Is it better to add taxa or characters to a difficult
856 phylogenetic problem? Syst. Biol. 47, 9–17.
857 Hatch, J.J., Brown, K.M., Hogan, G.G., Morris, R.D., 2000. Great Cormorant (Phalacrocorax
858 carbo). Birds N. Am. Online.
859 Hedtke, S.M., Townsend, T.M., Hillis, D.M., Collins, T., 2006. Resolution of phylogenetic
860 conflict in large data sets by increased taxon sampling. Syst. Biol. 55, 522–529.
861 Hernández-Mena, D.I., García-Prieto, L., García-Varela, M., 2014. Morphological and molecular
862 differentiation of *Parastrigea* (Trematoda: Strigeidae) from Mexico, with the description
863 of a new species. Parasitol. Int. 63, 315–323.
864 Hernández-Mena, D.I., García-Varela, M., Pérez-Ponce de León, G., 2017. Filling the gaps in the
865 classification of the Digenea Carus, 1863: systematic position of the
866 Proterodiplostomidae Dubois, 1936 within the superfamily Diplostomoidea Poirier, 1886,
867 inferred from nuclear and mitochondrial DNA sequences. Syst. Parasitol. 94, 833–848.
868 Hoffman, G.L., 1958. Experimental studies on the cercaria and metacercaria of a strigeoid
869 trematode, *Posthodiplostomum minimum*. Exp. Parasitol. 7, 23–50.
870 Howe, K.L., Bolt, B.J., Cain, S., Chan, J., Chen, W.J., Davis, P., Done, J., Down, T., Gao, S.,
871 Grove, C., Harris, T.W., Kishore, R., Lee, R., Lomax, J., Li, Y., Muller, H.-M.,
872 Nakamura, C., Nuin, P., Paulini, M., Raciti, D., Schindelman, G., Stanley, E., Tuli, M.A.,
873 Van Auken, K., Wang, D., Wang, X., Williams, G., Wright, A., Yook, K., Berriman, M.,
874 Kersey, P., Schedl, T., Stein, L., Sternberg, P.W., 2016. WormBase 2016: expanding to
875 enable helminth genomic research. Nucleic Acids Res. 44, D774–D780.
876 Hugghins, E.J., 1954a. Life history of a strigeid trematode, *Hysteromorpha triloba* (Rudolphi,
877 1819) Lutz, 1931. II. Sporocyst through adult. Trans. Am. Microsc. Soc. 73, 221-236.
878 Hugghins, E.J., 1954b. Life history of a strigeid trematode, *Hysteromorpha triloba* Rudolphi,
879 1819) Lutz, 1931. I. Egg and miracidium. Trans. Am. Microsc. Soc. 73, 1-15.
880 Hughes, R.C., 1929. Studies on the trematode family Strigeidae (Holostomidae), No. XIV: Two
881 new species of Diplostomula. Occas. Pap. Mus. Zool. 202, 1–29.
882 Inoue, J.G., Miya, M., Tsukamoto, K., Nishida, M., 2003. Basal actinopterygian relationships: a
883 mitogenomic perspective on the phylogeny of the “ancient fish.” Mol. Phylogenet. Evol.
884 26, 110–120.
885 Johnson, A.D., 1970. *Alaria mustelae*: Description of mesocercaria and key to related species.
886 Trans. Am. Microsc. Soc. 89, 250-253.

bioRxiv preprint doi: https://doi.org/10.1101/333518; this version posted May 30, 2018. The copyright holder for this preprint (which was not certified by peer review) is the author/funder, who has granted bioRxiv a license to display the preprint in perpetuity. It is made available under aCC-BY 4.0 International license.

887 Kalbe, M., Wegner, K.M., Reusch, T.B.H., 2016. Dispersion patterns of parasites in 0+ year
888 three-spined sticklebacks: a cross population comparison. J. Fish Biol. 60, 1529–1542.
889 Kostadinova, A., Pérez-del-Olmo, A., 2014. The Systematics of the Trematoda, in: Toledo, R.,
890 Fried, B. (Eds.), Digenetic Trematodes. Springer New York, New York, NY, pp. 21–44.
891 Kvach, Y., Jurajda, P., Bryjová, A., Trichkova, T., Ribeiro, F., Přikrylová, I., Ondračková, M.,
892 2017. European distribution for metacercariae of the North American digenean
893 *Posthodiplostomum* cf. *minimum centrarchi* (Strigeiformes: Diplostomidae). Parasitol.
894 Int. 66, 635–642.
895 Kvach, Y., Ondračková, M., Jurajda, P., 2016. First report of metacercariae of *Cyathocotyle*
896 *prussica* parasitising a fish host in the Czech Republic, Central Europe. Helminthologia
897 53, 1–5.
898 La Rue, G.R., 1957. The classification of Digenetic Trematoda: A review and a new system.
899 Exp. Parasitol. 6, 306–349.
900 Lapage, G., 1961. A list of the parasitic protozoa, helminths and Arthropoda recorded from
901 species of the family Anatidae (ducks, geese and swans). Parasitology 51, 1-109.
902 Locke, S.A., Al-Nasiri, F.S., Caffara, M., Drago, F., Kalbe, M., Lapierre, A.R., McLaughlin,
903 J.D., Nie, P., Overstreet, R.M., Souza, G.T., Takemoto, R.M., Marcogliese, D.J., 2015.
904 Diversity, specificity and speciation in larval Diplostomidae (Platyhelminthes: Digenea)
905 in the eyes of freshwater fish, as revealed by DNA barcodes. Int. J. Parasitol. 45, 841–
906 855.
907 Locke, S.A., McLaughlin, J.D., Lapierre, A.R., Johnson, P.T., Marcogliese, D.J., 2011. Linking
908 larvae and adults of *Apharyngostrigea cornu*, *Hysteromorpha triloba* and *Alaria mustelae*
909 (Diplostomoidea: Digenea) using molecular data. J. Parasitol. 97, 846–851.
910 Locke, S.A., McLaughlin, J.D., Marcogliese, D.J., 2010. DNA barcodes show cryptic diversity
911 and a potential physiological basis for host specificity among Diplostomoidea
912 (Platyhelminthes: Digenea) parasitizing freshwater fishes in the St. Lawrence River,
913 Canada. Mol. Ecol. 19, 2813–2827.
914 López-Hernández, D., Locke, S.A., de Melo, A.L., Leite Rabelo, E., Pinto, H.A., 2018.
915 Molecular, morphological and experimental assessment of the life cycle of
916 *Posthodiplostomum nanum* Dubois 1937 (Trematoda: Diplostomidae) from Brazil, with
917 phylogenetic evidence of paraphyly of the genus *Posthodiplostomum* Dubois, 1936.
918 Infect. Genet. Evol. In press. DOI: 10.1016/j.meegid.2018.05.010
919 López-Jiménez, A., Pérez-Ponce de León, G., García-Varela, M., 2017. Molecular data reveal
920 high diversity of *Uvulifer* (Trematoda: Diplostomidae) in Middle America, with the
921 description of a new species. J. Helminthol. In press. DOI: 10.1017/S0022149X17000888
922 Lunaschi, L.I., Cremonte, F., Drago, F.B., 2007. Checklist of digenean parasites of birds from
923 Argentina. Zootaxa 1403, 1-36.
924 Lunter, G., Goodson, M., 2011. Stampy: a statistical algorithm for sensitive and fast mapping of
925 Illumina sequence reads. Genome Res. 21, 936–939.
926 Lutz, A., 1931. Contribuição ao conhecimento da ontogenia das strigeidas. Mem. Inst. Oswaldo
927 Cruz 25, 333–342.
928 MacCallum, G., 1921. Studies in helminthology. Zoopathologica 1, 137–284.
929 McDonald, M.E., 1981. Key to Trematodes Reported in Waterfowl. US Fish and Wildlife
930 Service.
931 Moszczynska, A., Locke, S.A., McLaughlin, J.D., Marcogliese, D.J., Crease, T.J., 2009.
932 Development of primers for the mitochondrial cytochrome *c* oxidase I gene in digenetic

bioRxiv preprint doi: https://doi.org/10.1101/333518; this version posted May 30, 2018. The copyright holder for this preprint (which was not certified by peer review) is the author/funder, who has granted bioRxiv a license to display the preprint in perpetuity. It is made available under aCC-BY 4.0 International license.

933 trematodes (Platyhelminthes) illustrates the challenge of barcoding parasitic helminths.
934 Mol. Ecol. Resour. 9, 75–82.
935 Niewiadomska, K., 2002a. Superfamily Diplostomoidea, in: Gibson, D.I., Jones, A., Bray, R.
936 (Eds.), Keys to the Trematoda. CABI Publishing, Oxon, UK, pp. 159–166.
937 Niewiadomska, K., 2002b. Family Strigeidae Railliet, 1919, in: Gibson, D., Jones, A., Bray, R.
938 (Eds.), Keys to the Trematoda. CABI Publishing, Oxon, UK, pp. 231–241.
939 Niewiadomska, K., 2002c. Family Diplostomidae Poirier, 1886, in: Gibson, D.I., Jones, A., Bray,
940 R. (Eds.), Keys to the Trematoda. CABI Publishing, Oxon, UK, pp. 167–196.
941 Olson, P., Cribb, T., Tkach, V., Bray, R., Littlewood, D., 2003. Phylogeny and classification of
942 the Digenea (Platyhelminthes: Trematoda). Int. J. Parasitol. 33, 733–755.
943 Overstreet, R.M., Curran, S.S., Pote, L.M., King, D.T., Blend, C.K., Grater, W.D., 2002.
944 *Bolbophorus damnificus* n. sp. (Digenea: Bolbophoridae) from the channel catfish
945 *Ictalurus punctatus* and American white pelican *Pelecanus erythrorhynchos* in the USA
946 based on life-cycle and molecular data. Syst. Parasitol. 52, 81–96.
947 Palmieri, J.R., 1977. Host-induced morphological variations in the strigeoid trematode
948 *Posthodiplostomum minimum* (Trematoda: Diplostomatidae) II: Body measurements and
949 tegument modifications. Gt. Basin Nat. 37, 129–137.
950 Park, G.-M., 2007. Genetic comparison of liver flukes, *Clonorchis sinensis* and *Opisthorchis*
951 *viverrini*, based on rDNA and mtDNA gene sequences. Parasitol. Res. 100, 351–357.
952 Pearson, J.C., 1972. A phylogeny of life-cycle patterns of the Digenea. Adv. Parasitol. 10, 153–
953 189.
954 Pearson, J.C., Johnson, A.D., 1988. The taxonomic status of *Alaria marcianae* (Trematoda:
955 Diplostomidae). Proc. Helminthol. Soc. Wash. 55, 102–103.
956 Peng, Y., Leung, H.C., Yiu, S.-M., Chin, F.Y., 2012. IDBA-UD: a de novo assembler for single-
957 cell and metagenomic sequencing data with highly uneven depth. Bioinformatics 28,
958 1420–1428.
959 Perea, S., Vukić, J., Šanda, R., Doadrio, I., 2016. Ancient mitochondrial capture as factor
960 promoting mitonuclear discordance in freshwater fishes: A case study in the genus
961 *Squalius* (Actinopterygii, Cyprinidae) in Greece. PLOS ONE 11, e0166292.
962 Philippe, H., Brinkmann, H., Lavrov, D.V., Littlewood, D.T.J., Manuel, M., Wörheide, G.,
963 Baurain, D., 2011. Resolving difficult phylogenetic questions: Why more sequences are
964 not enough. PLoS Biol. 9, e1000602.
965 Platt, R.N., Faircloth, B.C., Sullivan, K.A., Kieran, T.J., Glenn, T.C., Vandewege, M.W., Lee,
966 T.E., Baker, R.J., Stevens, R.D., Ray, D.A., 2018. Conflicting evolutionary histories of
967 the mitochondrial and nuclear genomes in New World *Myotis* bats. Syst. Biol. 67, 236–
968 249.
969 Pleijel, F., Jondelius, U., Norlinder, E., Nygren, A., Oxelman, B., Schander, C., Sundberg, P.,
970 Thollesson, M., 2008. Phylogenies without roots? A plea for the use of vouchers in
971 molecular phylogenetic studies. Mol. Phylogenet. Evol. 48, 369–371.
972 Rudolphi, C., 1819. Entozoorum synopsis cui accedunt mantissima duplex et indices
973 locupletissima. Sumptibus Augusti Rücker, Berlin, Germany
974 Sattmann, H., Hörweg, C., Stagl, V., 2014. Johann Gottfried Bremser (1767–1827) und die
975 Kuhpockenimpfung. Wien. Klin. Wochenschr. 126, 3–10.
976 Sereno-Uribe, A.L., López-Jimenez, A., Andrade-Gómez, L., García-Varela, M., 2018. A
977 morphological and molecular study of adults and metacercariae of *Hysteromorpha triloba*

bioRxiv preprint doi: https://doi.org/10.1101/333518; this version posted May 30, 2018. The copyright holder for this preprint (which was not certified by peer review) is the author/funder, who has granted bioRxiv a license to display the preprint in perpetuity. It is made available under aCC-BY 4.0 International license.

(Rudolpi, 1819), Lutz 1931 (Diplostomidae) from the Neotropical region. J. Helminthol. In press. DOI: 10.1017/S0022149X17001237

Shoop, W.L., 1989. Systematic analysis of the Diplostomidae and Strigeidae (Trematoda). J. Parasitol. 75, 21–32.

Silvestro, D., Michalak, I., 2012. raxmlGUI: a graphical front-end for RAxML. Org. Divers. Evol. 12, 335–337.

Simão, F.A., Waterhouse, R.M., Ioannidis, P., Kriventseva, E.V., Zdobnov, E.M., 2015. BUSCO: assessing genome assembly and annotation completeness with single-copy orthologs. Bioinformatics btv351.

Stamatakis, A., 2014. RAxML version 8: a tool for phylogenetic analysis and post-analysis of large phylogenies. Bioinformatics 30, 1312–1313.

Stoyanov, B., Georgieva, S., Pankov, P., Kudlai, O., Kostadinova, A., Georgiev, B.B., 2017. Morphology and molecules reveal the alien *Posthodiplostomum centrarchi* Hoffman, 1958 as the third species of *Posthodiplostomum* Dubois, 1936 (Digenea: Diplostomidae) in Europe. Syst. Parasitol. 94, 1–20.

Stunkard, H.W., 1946. Interrelationships and taxonomy of the digenetic trematodes. Biol. Rev. 21, 148–158.

Sun, M., Soltis, D.E., Soltis, P.S., Zhu, X., Burleigh, J.G., Chen, Z., 2015. Deep phylogenetic incongruence in the angiosperm clade Rosidae. Mol. Phylogenet. Evol. 83, 156–166.

Tamura, K., Stecher, G., Peterson, D., Filipski, A., Kumar, S., 2013. MEGA6: Molecular Evolutionary Genetics Analysis version 6.0. Mol. Biol. Evol. 30, 2725–2729.

Uhrig, E.J., Spagnoli, S.T., Tkach, V.V., Kent, M.L., Mason, R.T., 2015. *Alaria* mesocercariae in the tails of red-sided garter snakes: evidence for parasite-mediated caudectomy. Parasitol. Res. 114, 4451–4461.

Waeschenbach, A., Webster, B.L., Littlewood, D.T.J., 2012. Adding resolution to ordinal level relationships of tapeworms (Platyhelminthes: Cestoda) with large fragments of mtDNA. Mol. Phylogenet. Evol. 63, 834–847.

Whitfield, J.B., Lockhart, P.J., 2007. Deciphering ancient rapid radiations. Trends Ecol. Evol. 22, 258–265.

Zeder, J., 1800. Erster Nachtrag zur Naturgeschichte der Eingeweidewürmer. Leipzig.

Table 1. Origins of samples and data in the present and other studies

	Locality	Source	CO1 accession	UCE accession	Mt genome accession	rDNA operon accession	Museum accession
Diplostomoidea Poirier, 1886							
Diplostomidae Poirier, 1886							
Alaria Schrank, 1788							
Alaria americana Hall and Wigdor, 1918							
Vulpes vulpes	Nova Scotia, Canada	present study	XXXXXXX	XXXXXX	XXXXXX	XXXXXXX	XXXXXXX
Lithobates clamitans	Quebec, Canada	present study	XXXXXXX				
Alaria marcianae (La Rue, 1917)							
Taxidea taxus, Thamnophis sirtalis parietalis	North Dakota, USA; Manitoba, Canada	Uhrig et al	KT254037-9				
Anaxyrus boreas, Lithobates catesbeiana, Pseudacris regilla	California, USA	Locke et al 2011	JF769440-8, JF904530-6				
Alaria mustelae Bosma, 1931							
Martes pennanti	Wisconsin, USA	present study	XXXXXXX-X				
Neovison vison, L. clamitans, Lithobates pipiens	New Hampshire, USA; Ontario, Quebec, Canada	Locke et al 2011	FJ477182, JF769422-437, JF904528-9				
Hysteromorpha Lutz, 1931							
Hysteromorpha triloba (Rudolphi, 1819)							
Squalius cephalus	Emilia Romagna, Italy	present study	XXXXXXX	XXXXXX	XXXXXX	XXXXXXX	XXXXXXX

bioRxiv preprint doi: https://doi.org/10.1101/333518; this version posted May 30, 2018. The copyright holder for this preprint (which was not certified by peer review) is the author/funder, who has granted bioRxiv a license to display the preprint in perpetuity. It is made available under aCC-BY 4.0 International license.

Table 1. Origins of samples and data in the present and other studies

	Locality	Source	CO1 accession	UCE accession	Mt genome accession	rDNA operon accession	Museum accession
Hysteromorpha corti (Hughes, 1929)							
Phalacrocorax auritus, Catostomus commersoni, Ictalurus nebulosus, Notemigonus crysoleucas	Ontario, Quebec, Nova Scotia, Canada; Florida, USA	Locke et al 2011, present study	XXXXXX, FJ477203, HM064712, HM064714-17, JF769457-76				
Nannopterum brasilianus, Astyanax mexicanus	San Luis Potosi, Chiapas, Veracruz, Mexico	Sereno-Uribe et al 2017	MG649464-78				
Posthodiplostomum Dubois, 1936							
Posthodiplostomum centrarchi Hoffman, 1958							
Ardea herodias	Montreal, Quebec, Canada	present study	XXXXXXX	XXXXXX	XXXXXX	XXXXXXX	XXXXXXX
Lepomis microlophus	Puerto Rico	present study	XXXXXXX				
A. herodias, Lepomis gibbosus, Ambloplites rupestris	Quebec, Canada	Locke et al 2010	FJ477217, HM064799-807, HM064809-24, HM064826-43				

bioRxiv preprint doi: https://doi.org/10.1101/333518; this version posted May 30, 2018. The copyright holder for this preprint (which was not certified by peer review) is the author/funder, who has granted bioRxiv a license to display the preprint in perpetuity. It is made available under aCC-BY 4.0 International license.

Table 1. Origins of samples and data in the present and other studies

	Locality	Source	CO1 accession	UCE accession	Mt genome accession	rDNA operon accession	Museum accession
Ardea cinerea, L. gibbosus	Spain, Slovakia, Bulgaria	Stoyanova et al. 2017	KX931421-3				
Tylodelphys Diesing, 1850							
Tylodelphys immer Dubois, 1961							
Gavia immer	Quebec, Canada	present study		XXXXXX	XXXXXX	XXXXXXX	XXXXXXX
G. immer, Coregonus clupeaformis, Notropis hudsonius, Perca flavescens, Salvelinus fontinalis	Quebec, Canada	Locke et al. 2015	KR271481-93				
Strigeidae Railliet, 1919							
Cardiocephaloides Sudarikov, 1959							
Cardiocephaloides medioconiger Dubois and Vigueras, 1949							
Thallasius maximus	Florida, USA	present study	XXXXXXX	XXXXXX	XXXXXX	XXXXXXX	XXXXXXX
Larus sp.	Campeche, Mexico	Hernandez-Mena Parasitol. Int. 63 (2), 315-323 (2014)	JX977782-3				
Cardiocephaloides sp.							
Larus occidentalis	Baja California, Mexico	Hernandez-Mena Parasitol. Int. 63 (2), 315-323 (2014)	JX977784				
Cotylurus Szidat, 1928							
Cotylurus marcogliese n. sp.							
Lophodytes cucullatus	Montreal, Quebec,	present study	XXXXXXXX	XXXXXXX	XXXXXXX	XXXXXXX	XXXXXXX

bioRxiv preprint doi: https://doi.org/10.1101/333518; this version posted May 30, 2018. The copyright holder for this preprint (which was not certified by peer review) is the author/funder, who has granted bioRxiv a license to display the preprint in perpetuity. It is made available under aCC-BY 4.0 International license.

Table 1. Origins of samples and data in the present and other studies

	Locality	Source	CO1 accession	UCE accession	Mt genome accession	rDNA operon accession	Museum accession
	Canada						
Cotylurus cornutus (Rudolphi, 1808)							
Gyraulus acronicus, Radix balthica	Lake Takvatn, Norway	Soldanova et al 2017 Int J Parasitol	KY513231-6				
Cotylurus gallinulinae (Lutz, 1928)							
Aythya affinis	Sonora, Mexico	Hernandez-Mena Parasitol. Int. 63 (2), 315-323 (2014)	JX977781				
Cotylurus flabelliformis (Faust, 1917)							
Aythya vallisneria	Manitoba, Canada	present study	XXXXXXX				XXXXXXX
Cotylurus strigeoides Dubois, 1958							
Aythya collaris	Manitoba, Canada	present study	XXXXXXX				XXXXXXX
Cyathocotylidae Mühling, 1888							
Cyathocotyle Mühling, 1896							
Cyathocotyle prussica Mühling, 1896							
Gasterosteus aculeatus	Germany	present study		XXXXXX	XXXXXX	XXXXXXX	
G. aculeatus	Germany	Blasco-Costa and Locke, 2017	XXXXXXX				

bioRxiv preprint doi: https://doi.org/10.1101/333518; this version posted May 30, 2018. The copyright holder for this preprint (which was not certified by peer review) is the author/funder, who has granted bioRxiv a license to display the preprint in perpetuity. It is made available under aCC-BY 4.0 International license.

Table 1. Origins of samples and data in the present and other studies

	Locality	Source	CO1 accession	UCE accession	Mt genome accession	rDNA operon accession	Museum accession
Mesostephanus Lutz, 1935							
Mesostephanus microbursa Caballero, Grocott, and Zerecero, 1953							
Sula nebouxii	Nayarit, Mexico	Hernandez-Mena et al 2017	MF398316				
Mesostephanus sp.							
L. gibbosus, Pomoxis nigromaculatus	Quebec, Canada	Locke et al. 2010	HM064651, HM064653-9				
Brauninidae Wolf 1903							
Braunina Heider, 1900							
Braunina cordiformis Wolf, 1903							
Delphinus delphis	Coastal waters, Argentina	Blasco-Costa and Locke, 2017	MF124272				

bioRxiv preprint doi: https://doi.org/10.1101/333518; this version posted May 30, 2018. The copyright holder for this preprint (which was not certified by peer review) is the author/funder, who has granted bioRxiv a license to display the preprint in perpetuity. It is made available under aCC-BY 4.0 International license.

Table 2. Selected assembly statistics for 150-bp paired-end reads from IDBA_hybrid.

	Reads	Aligned reads	Expected coverage	Contigs	N50	max	mean	Total length	N80
Cyathocotylidae									
Cyathocotyle prussica	21208232	7029966	0.055976	336463	542	13687	522	175748574	396
Strigeidae									
Cardiocephaloides medioconiger	91513844	72475903	0.120399	566427	11122	157631	1204	682202373	2185
Cotylurus marcogliesei n. sp.	136959212	80825403	0.133569	2065313	1662	217472	427	883621846	204
Diplostomidae									
Alaria americana	130527714	71565054	0.072403	1899210	1540	90097	658	1249851331	507
Hysteromorpha triloba	130953814	78792229	0.076501	1923782	1675	89784	675	1299457195	496
Posthodiplostomum centrarchi	143789074	81923449	0.105401	2157712	1245	878066	497	1074511666	329
Tylodelphys immer	123480600	80297700	0.155342	1736417	2044	382985	432	751015059	201

bioRxiv preprint doi: https://doi.org/10.1101/333518; this version posted May 30, 2018. The copyright holder for this preprint (which was not certified by peer review) is the author/funder, who has granted bioRxiv a license to display the preprint in perpetuity. It is made available under aCC-BY 4.0 International license.

bioRxiv preprint doi: https://doi.org/10.1101/333518; this version posted May 30, 2018. The copyright holder for this preprint (which was not certified by peer review) is the author/funder, who has granted bioRxiv a license to display the preprint in perpetuity. It is made available under aCC-BY 4.0 International license.

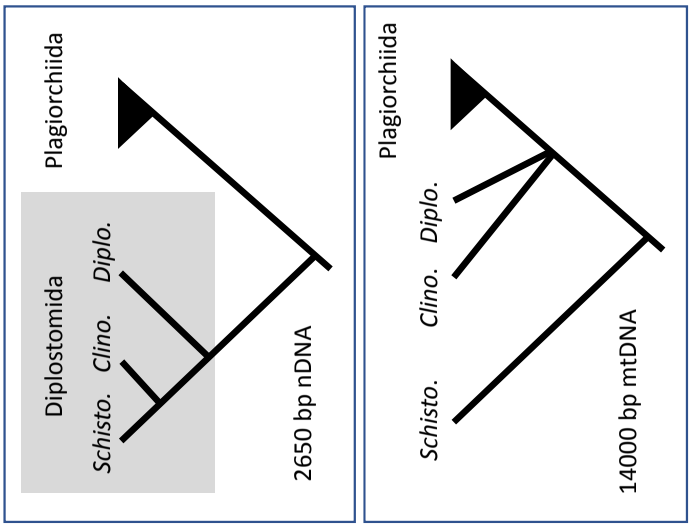

bioRxiv preprint doi: https://doi.org/10.1101/333518; this version posted May 30, 2018. The copyright holder for this preprint (which was not certified by peer review) is the author/funder, who has granted bioRxiv a license to display the preprint in perpetuity. It is made available under aCC-BY 4.0 International license.

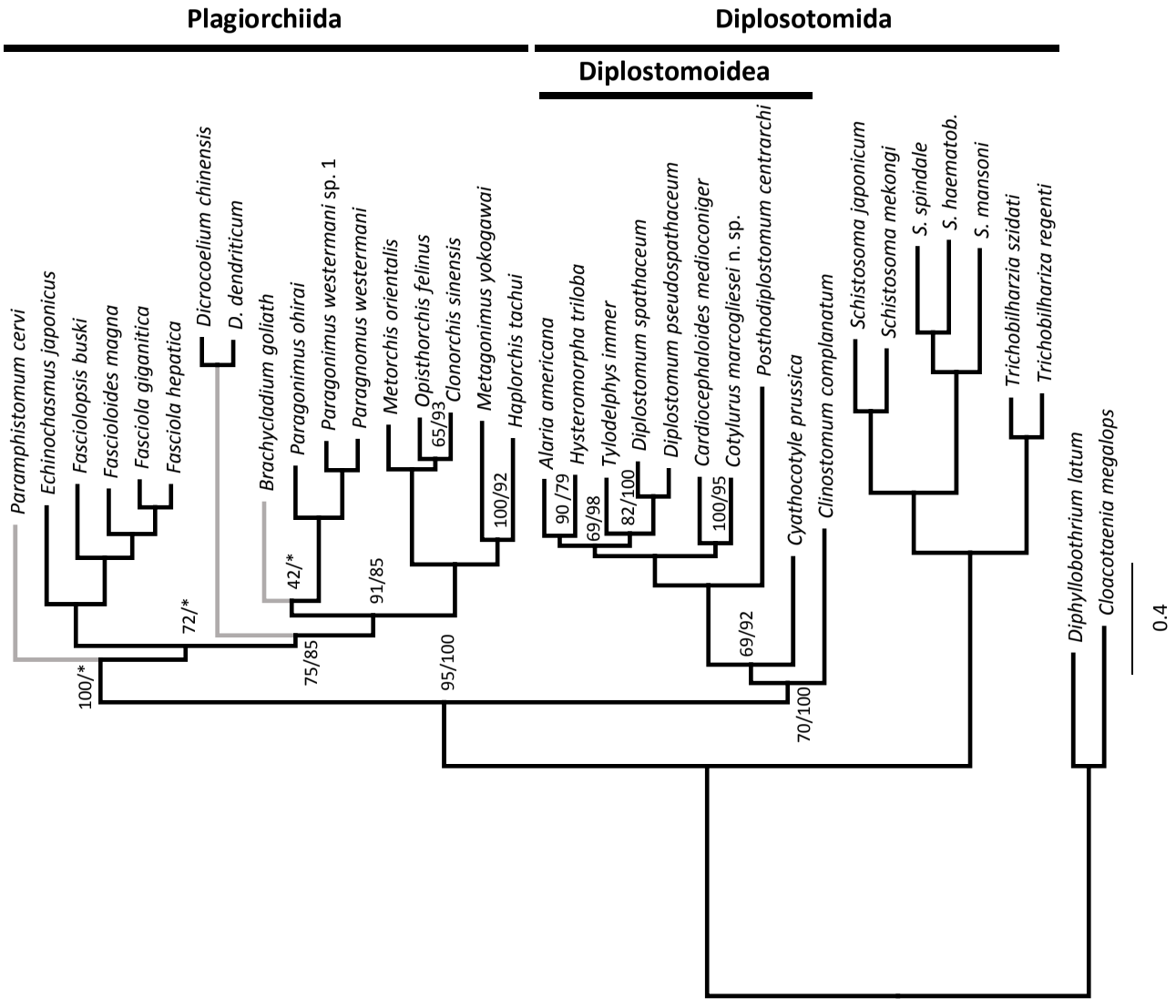

bioRxiv preprint doi: https://doi.org/10.1101/333518; this version posted May 30, 2018. The copyright holder for this preprint (which was not certified by peer review) is the author/funder, who has granted bioRxiv a license to display the preprint in perpetuity. It is made available under aCC-BY 4.0 International license.

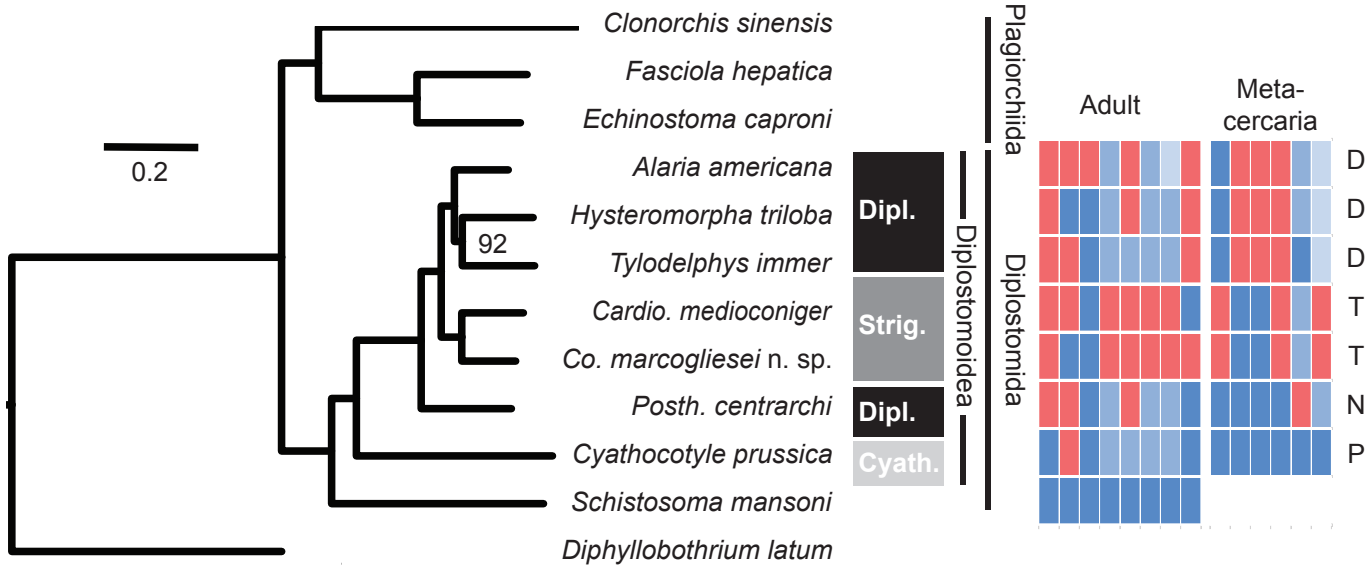

bioRxiv preprint doi: https://doi.org/10.1101/333518; this version posted May 30, 2018. The copyright holder for this preprint (which was not certified by peer review) is the author/funder, who has granted bioRxiv a license to display the preprint in perpetuity. It is made available under a CC BY 4.0 International license.

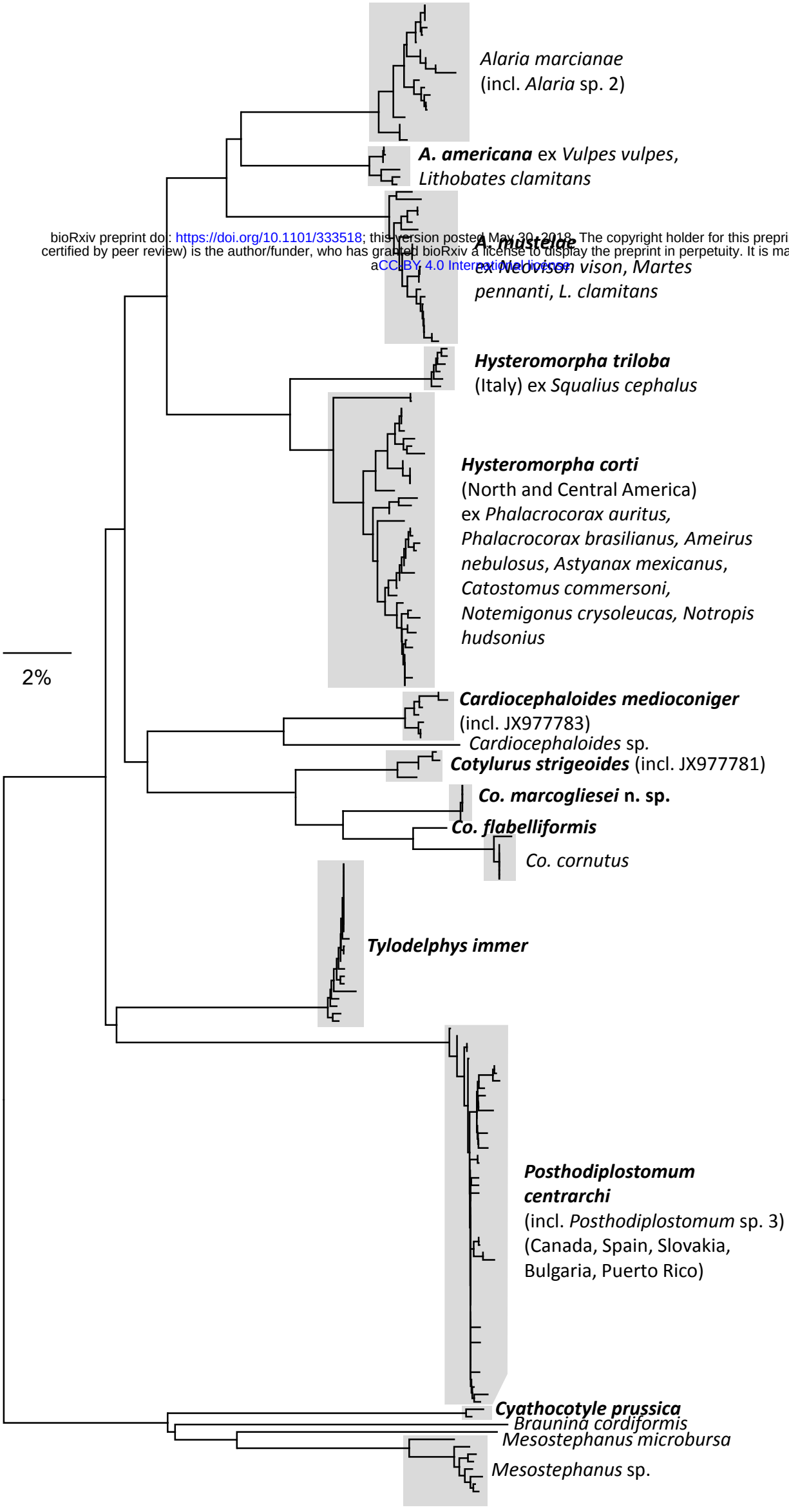

bioRxiv preprint doi: https://doi.org/10.1101/333518; this version posted May 30, 2018. The copyright holder for this preprint (which was not certified by peer review) is the author/funder, who has granted bioRxiv a license to display the preprint in perpetuity. It is made available under aCC-BY 4.0 International license.

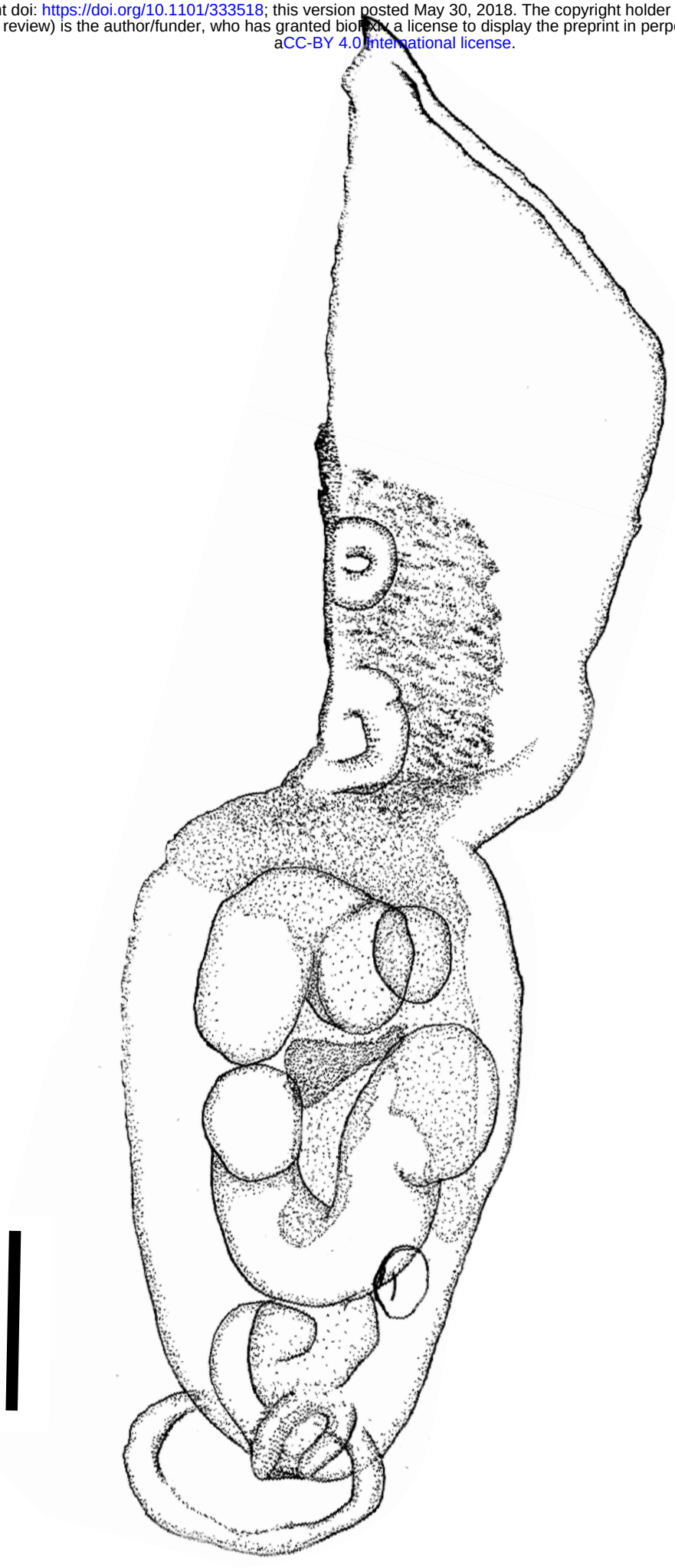

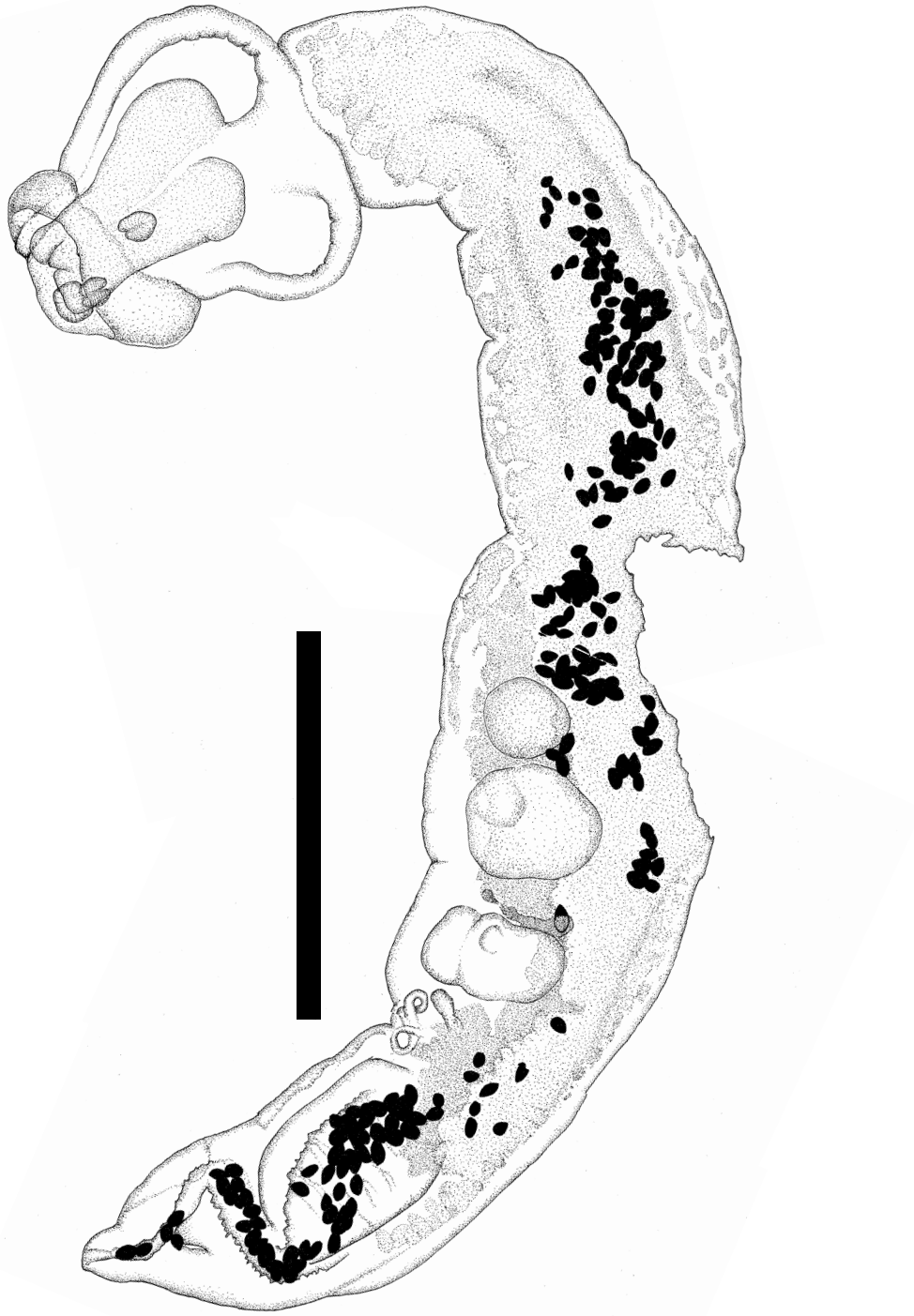

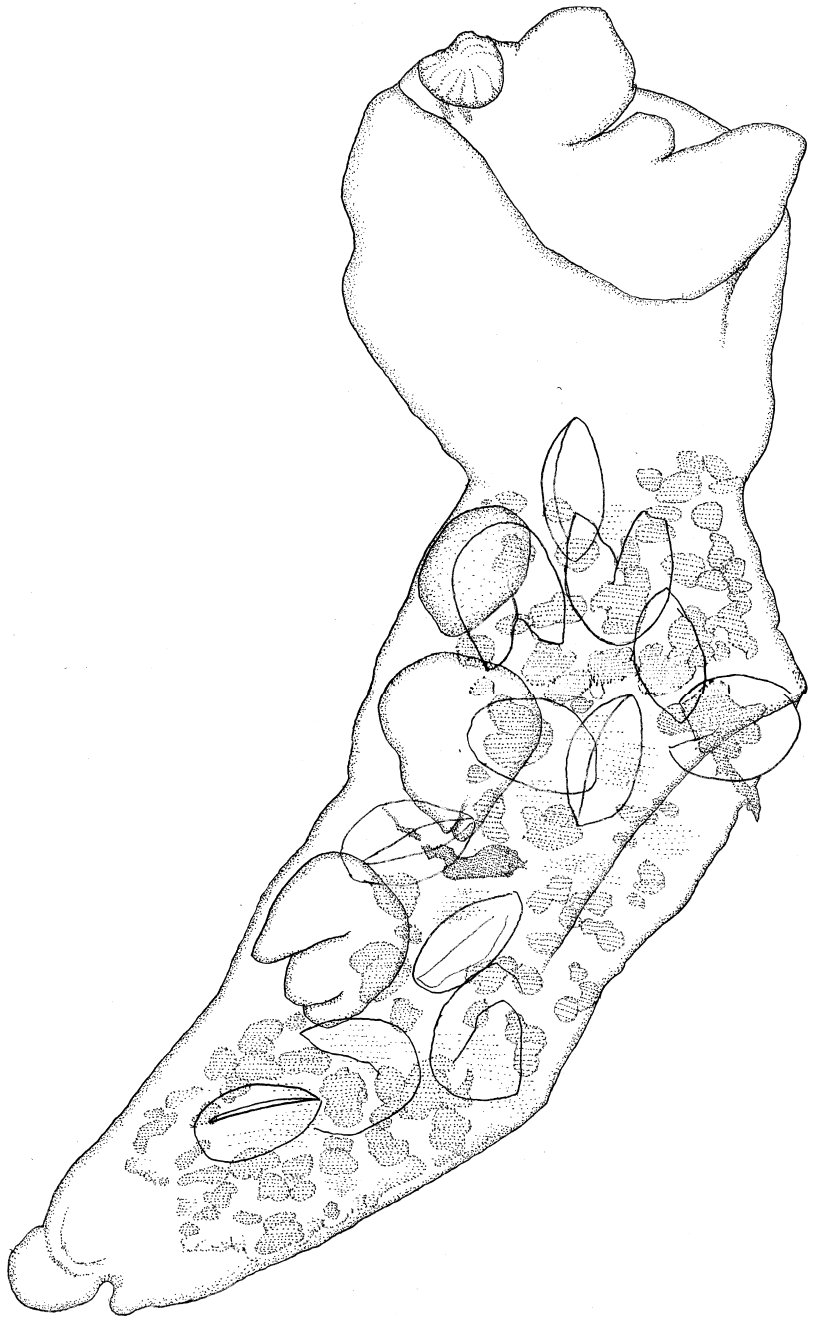

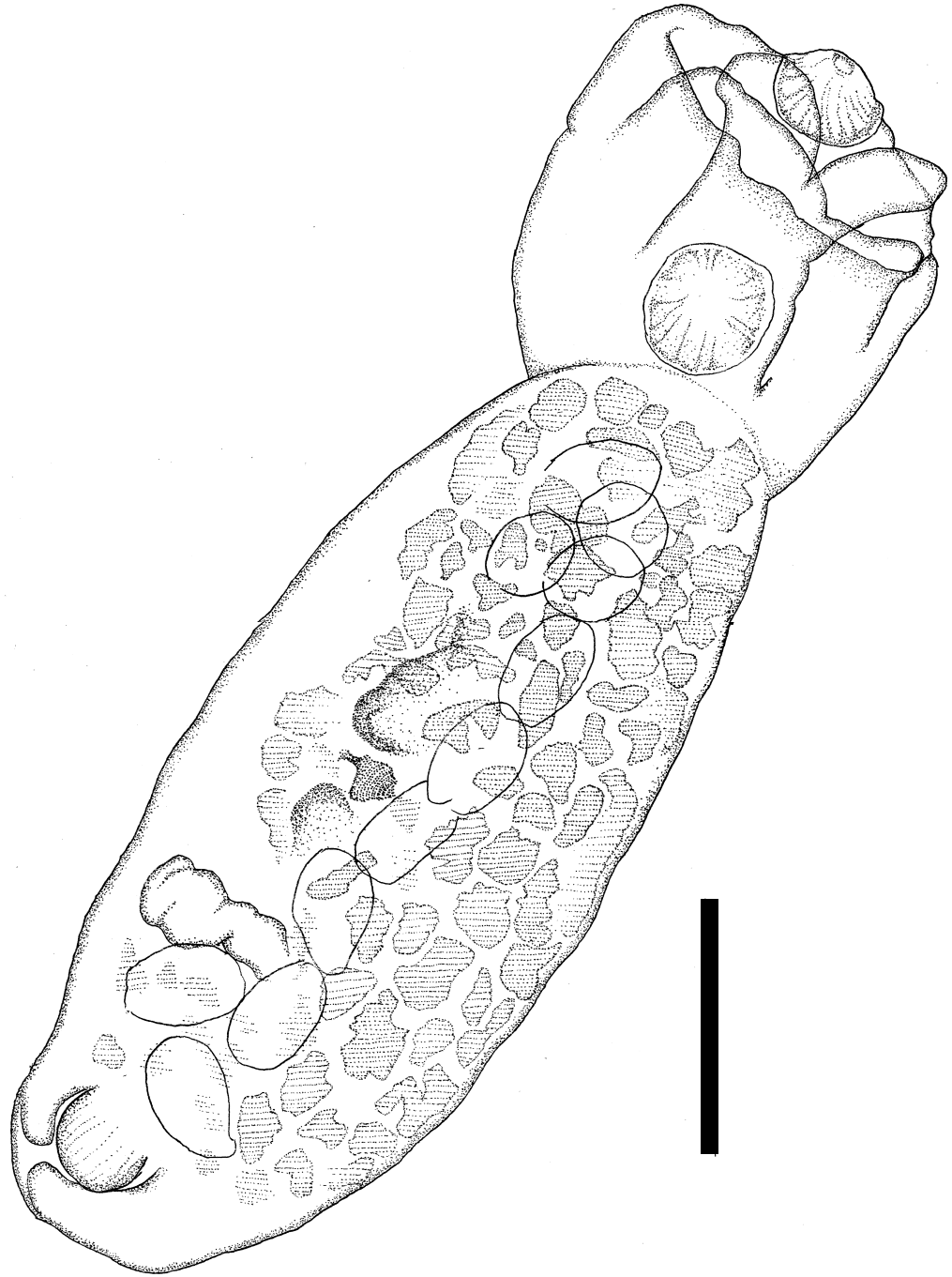

bioRxiv preprint doi: https://doi.org/10.1101/333518; this version posted May 30, 2018. The copyright holder for this preprint (which was not certified by peer review) is the author/funder, who has granted bioRxiv a license to display the preprint in perpetuity. It is made available under aCC-BY 4.0 International license.

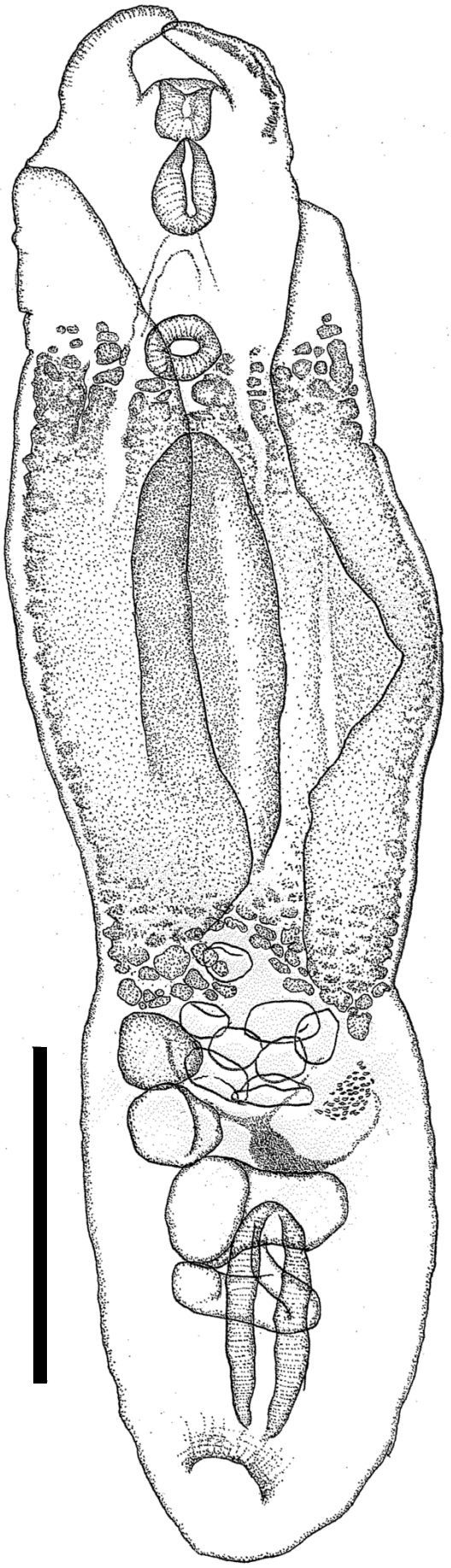

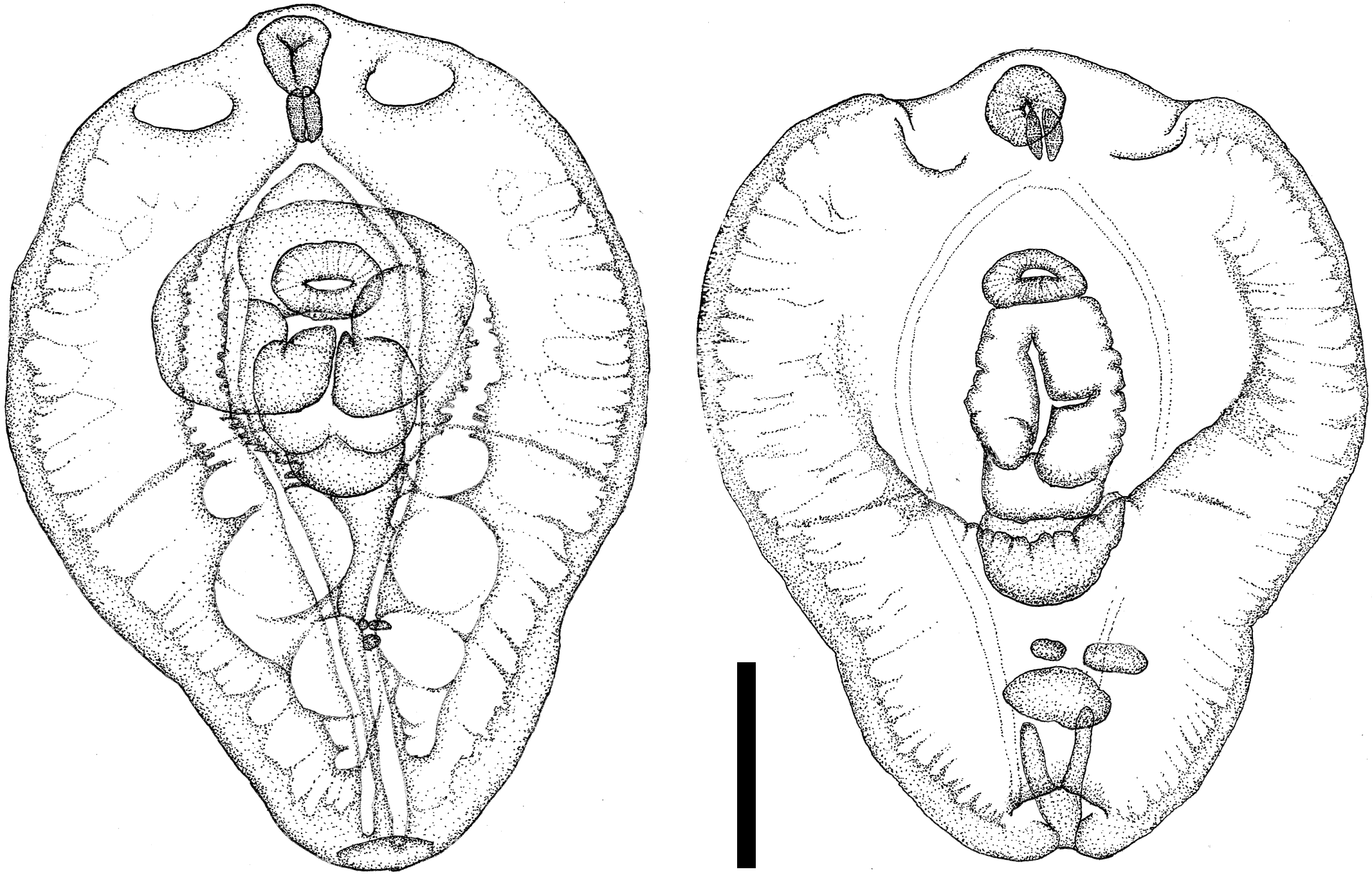

bioRxiv preprint doi: https://doi.org/10.1101/333518; this version posted May 30, 2018. The copyright holder for this preprint (which was n
certified by peer review) is the author/funder, who has granted bioRxiv a license to display the preprint in perpetuity. It is made available u
aCC-BY 4.0 International license.

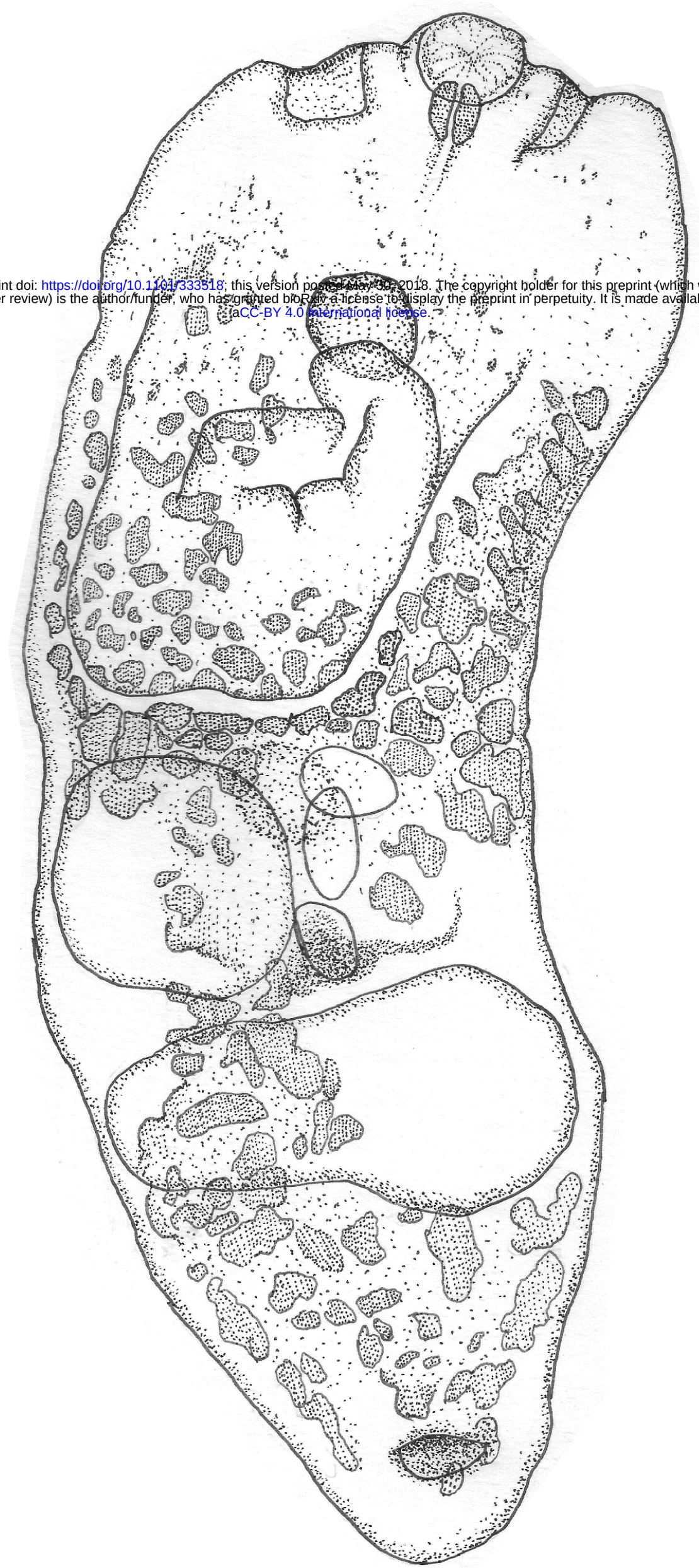

bioRxiv preprint doi: https://doi.org/10.1101/333518; this version posted May 30, 2018. The copyright holder for this preprint (which was not certified by peer review) is the author/funder, who has granted bioRxiv a license to display the preprint in perpetuity. It is made available under aCC-BY 4.0 International license.

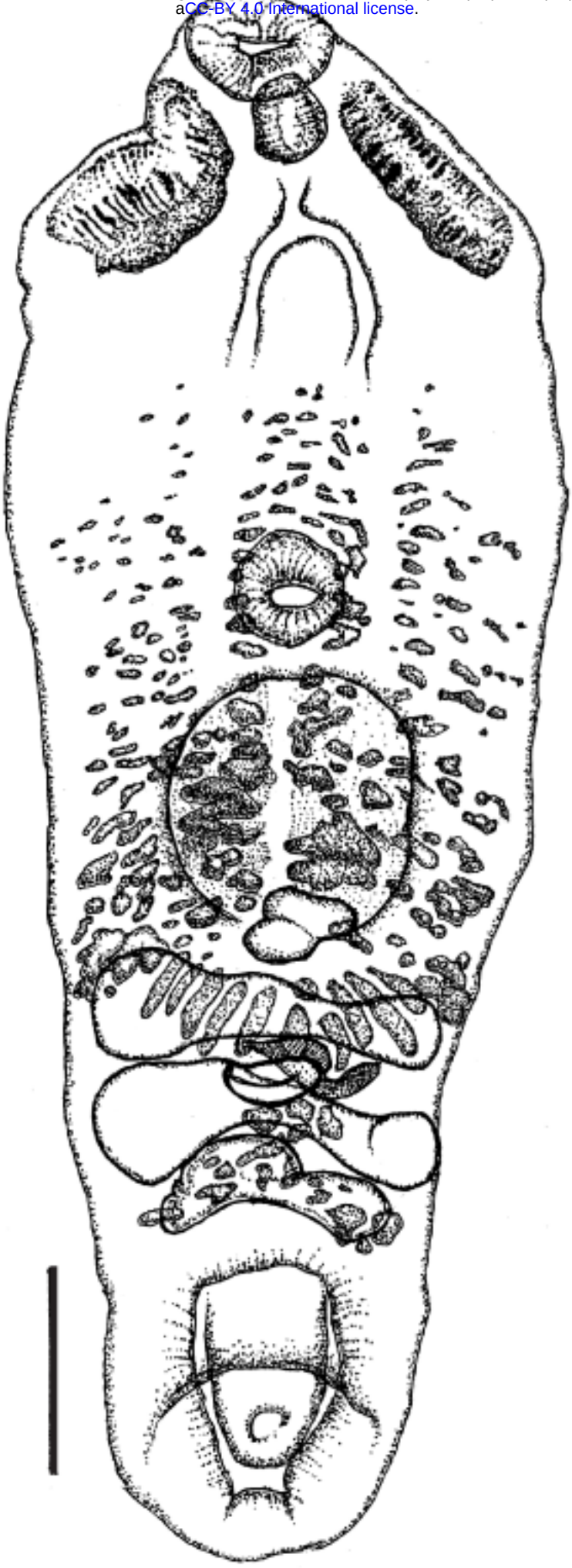

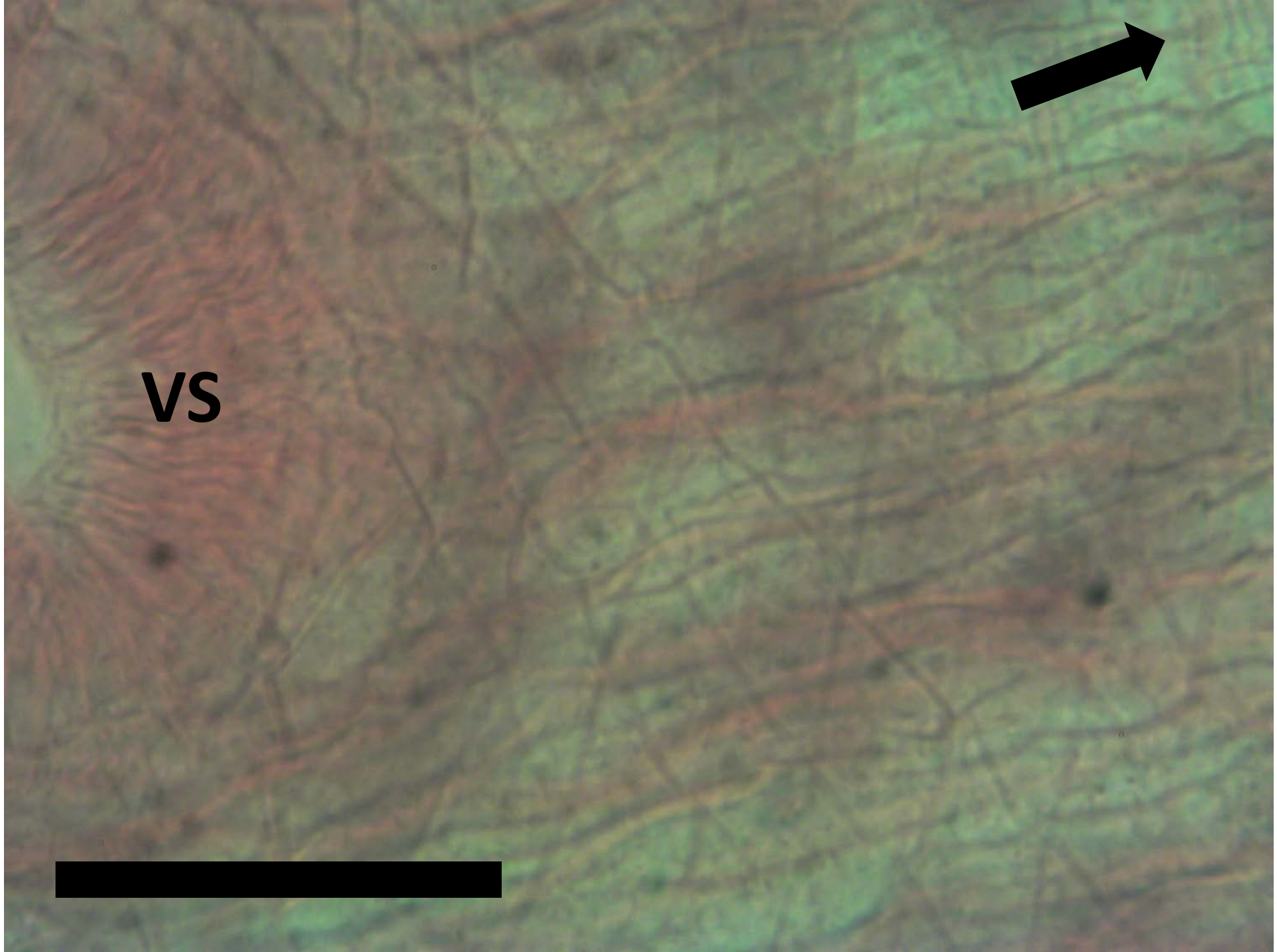
VS

Supplementary Figure 1. Characters mapped onto the topology of the phylogenomic analysis of the Diplostomoidea. Characters 1-10 were not included in the published figure because they are invariant within the Diplostomoidea

	Adult																		Metacercaria					
Character	1	2	3	4	5	6	7	8	9	10	11	12	13	14	15	16	17	18	19	20	21	22	23	24
Schistosoma mansoni	0	0	0	0	0	0	0	0	0	0	0	0	0	0	0	0	0	0						
Cyathocotyle prussica	3	3	3	3	3	3	3	3	3	3	0	3	0	1	1	1	1	0	0	0	0	0	0	0
Posthodiplostomum centrarchi	3	3	3	3	3	3	3	3	3	3	3	3	0	1	3	1	1	0	0	0	0	0	3	1
Cardiocephaloides medioconiger	3	3	3	3	3	3	3	3	3	3	3	3	0	3	3	3	3	0	3	0	0	3	1	3
Cotylurus marcogliesei	3	3	3	3	3	3	3	3	3	3	3	0	0	3	3	3	3	3	3	0	0	3	1	3
Alaria americana	3	3	3	3	3	3	3	3	3	3	3	3	3	1	3	1	2	3	0	3	3	3	1	2
Hysteromorpha triloba	3	3	3	3	3	3	3	3	3	3	3	0	0	1	3	1	1	3	0	3	3	3	1	2
Tylodelphys immer	3	3	3	3	3	3	3	3	3	3	3	3	0	1	1	1	1	3	0	3	3	3	0	2

Character

Adult

1 0=dioecious; 3=monoecious
2 0=testes>2; 3=testes 2
3 0=cirrus sac absent; 3=cirrus sac present
4 0=hermaphroditic duct present; 3=hermaphroditic duct absent
5 0=genital pore median; 3= gential pore terminal/sub-terminal
6 0=infection site of adult is gut; 3=infection site of adult is outside gut
7 0=testes non-spherical; 3=testes spherical
8 0=testes tandem; 3=testes opposite
9 0=pharynx absent; 3=pharynx present
10 0=metacercaria absent; 3=metacercaria present
11 0=genital bursa absent; 3=genital bursa present
12 0=genital cone absent; 3=genital cone present
13 0=mesocercaria absent; 3=mesocercaria present
14 0=tribocytic organ absent; 1=tribocytic organ lingual; 3=tribocytic organ bilobate
15 0=body shape unsegment; 1=slightly segnmented; 3=fore/hindbody division
16 0=no forebody; 1=flattenned forebody; 3=cup-shaped forebody
17 0=vitellaria postovarian in hindbody; 1= vitellaria pre- and post ovarian in fore and hindbody; 2=vitellaria pre-ovarian in forebody; 3=vitellaria pre- and postavarian in hindbody only
18 0=pseudosuckers absent; 3=pseudosuckers present

Metacercaria

19 0=forebody spathulate; 3=forebody cup-shaped
20 0=encysted; 3=unencysted
21 0=limebodies free; 3=limebodies enclosed
22 0=pseudosuckers present; 3=pseudosuckers absent
23 0=none; 1=no or weak segmentation; 3=segmented
24 0=four excretory canals in two loops; 1=1 median flanked by two lateral canals; 2=one median flanked by 1 in anterior, and 2 in posterior of median anastomosis; 3=net-like web of canals

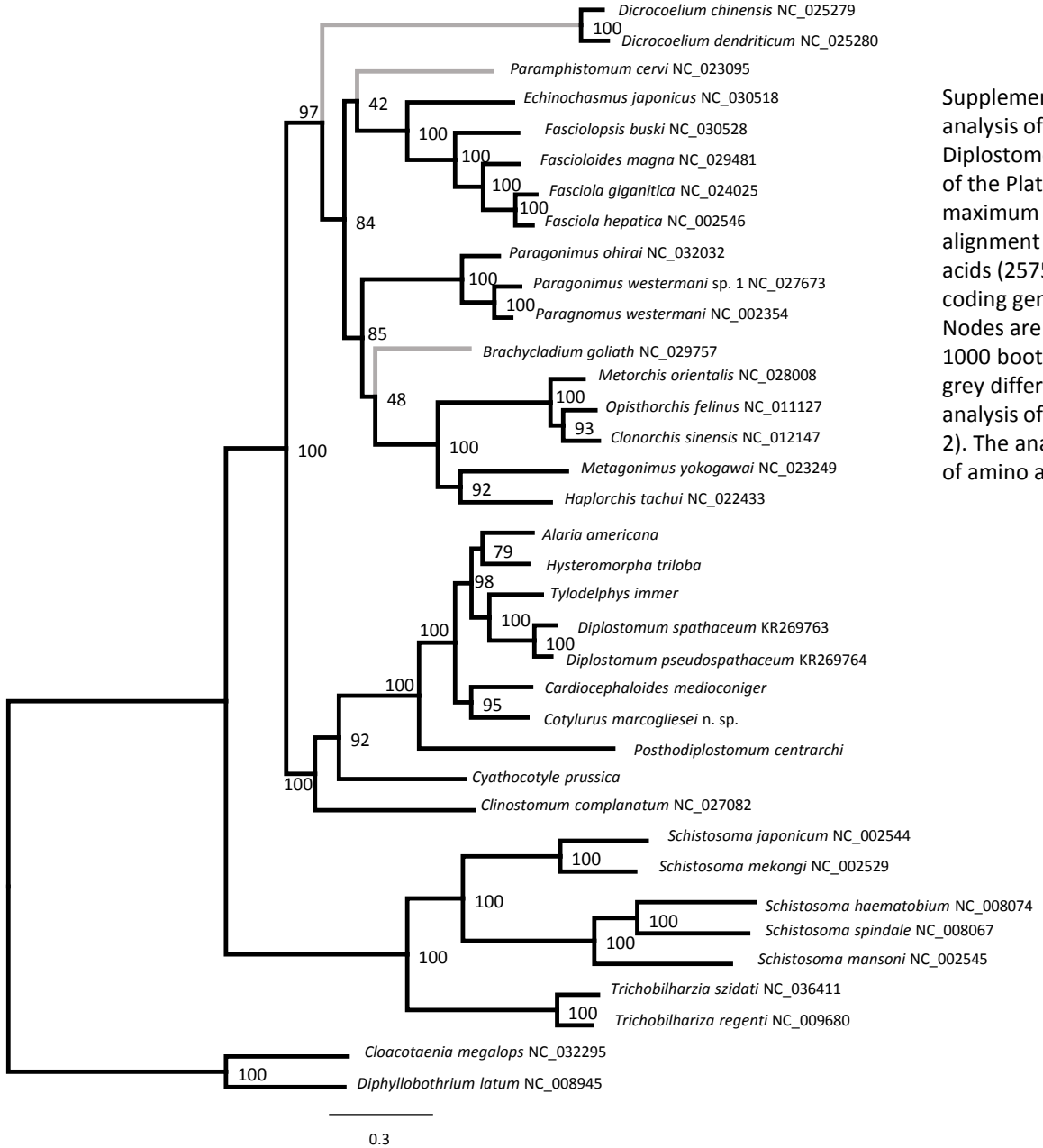

Supplementary Fig 2. Phylogenetic analysis of seven representatives of the Diplostomoidea and 29 other members of the Platyhelminthes, estimated using maximum likelihood based on an alignment of 3153 translated amino acids (2575 variable sites) in 13 protein-coding genes in the mitochondrion. Nodes are labelled with support from 1000 bootstrap replicates. Branches in grey differ from the topology in the analysis of nucleotide sequences (Figure 2). The analysis was based on JTT model of amino acid evolution.

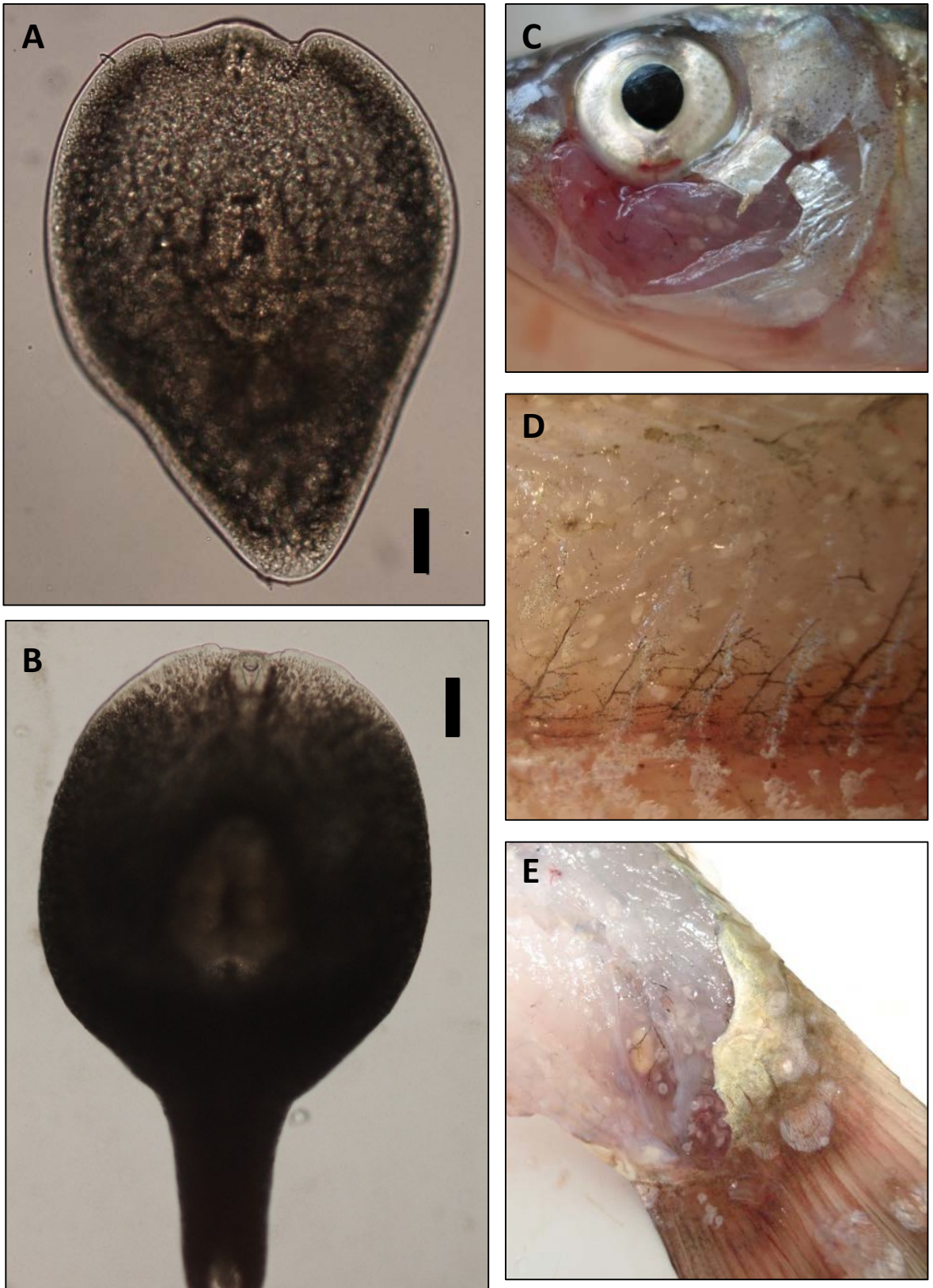

Supplementary Figure 3. Metacercaraie of *Hysteromorpha triloba* in muscle of *Squalius cephalus*. **A-B**: live metacercariae (scale = 100 μm); Metacercariae in cheek (**C**), lateral (**D**) and caudal (**E**) muscle.

bioRxiv preprint doi: https://doi.org/10.1101/333518; this version posted May 30, 2018. The copyright holder for this preprint (which was not certified by peer review) is the author/funder, who has granted bioRxiv a license to display the preprint in perpetuity. It is made available under aCC-BY 4.0 International license.

Supplementary Table 1. Characteristics and genomic assembly statistics of mitochondrial genomes and rDNA operons for seven members of the Diplostomoidea

	Tylodelphys immer			***Posthodiplostomum centrarchi***		
	14,193 bp (14,634 reads)			**14,561 bp (177, 166 reads)**		
Mitochondrial DNA	**start**	**stop**	**length**	**start**	**stop**	**length**
cox3	1	655	655	1	652	652
trnH(gtg)	680	746	67	686	746	61
cob	750	1,871	1,122	747	1,859	1,113
nad4l	1,861	2,124	264	1,863	2,126	264
nad4	2,085	3,380	1,296	2,087	3,385	1,299
trnQ(ttg)	3,382	3,446	65	3,403	3,464	62
trnF(gaa)	3,454	3,518	65	3,469	3,523	55
trnM(cat)	3,589	3,656	68	3,531	3,596	66
atp6	3,660	4,178	519	3,598	4,119	522
nad2	4,180	5,139	960	4,106	5,032	927
trnV(tac)	5,090	5,153	64	5,031	5,093	63
trnA(tgc)	5,162	5,225	64	5,094	5,157	64
trnD(gtc)	5,233	5,297	65	5,159	5,222	64
nad1	5,295	6,209	915	5,247	6,161	915
trnP(tgg)	6,215	6,281	67	6,169	6,230	62
trnN(gtt)	6,288	6,353	66	6,240	6,307	68
trnI(gat)	6,367	6,432	66	6,316	6,381	66
trnK(ctt)	6,434	6,501	68	6,383	6,447	65
nad3	6,506	6,862	357	6,453	6,809	357
tRNA-Ser	6,882	6,941	60	6,809	6,870	62
trnW(tca)	6,953	7,017	65	6,872	6,937	66
cox1	7,027	8,691	1,665	6,986	8,569	1,584
tRNA-Thr	8,780	8,848	69	8,584	8,649	66
trnT(tgt)						
large subunit rRNA	8,850	9,827	978	8,651	9,628	978
trnC(gca)	9,828	9,894	67	9,629	9,694	66
rrnS	9,892	10,634	743	9,693	10,423	731
cox2	10,662	11,276	615	10,455	11,060	606
nad6	11,291	11,752	462	11,060	11,518	459
trnY(gta)	11,768	11,831	64	11,529	11,593	65
trnL1(aag)	11,833	11,899	67	11,599	11,667	69
trnS2(tga)	11,900	11,965	66	11,668	11,732	65
trnL2(taa)	12,011	12,077	67	11,741	11,803	63
trnR(tcg)	12,097	12,166	70	11,808	11,877	70
nad5	12,166	13,755	1,590	11,877	13,463	1,587
trnE(ttc)	13,764	13,830	67	13,488	13,552	65
trnG(tcc)	14,120	14,190	71	14,496	14,560	65
Nuclear rDNA operon	**8032 bp (574,971 reads)**			**7787 bp (674,595 reads)**		
external transcribed spacer	1	764	764	1	535	535
small subunit rRNA	765	2,743	1,979	537	2514	1978
internal transcribed spacer 1	2,743	3,356	614	2515	3118	604
5.8S rRNA	3,357	3,513	157	3119	3275	157
internal transcribed spacer 2	3,514	3,808	295	3276	3561	286
large subunit rRNA	3,809	8,015	4,207	3562	7770	4209
external transcribed spacer	8,016	>8032	>17	7771	>7787	>17

bioRxiv preprint doi: https://doi.org/10.1101/333518; this version posted May 30, 2018. The copyright holder for this preprint (which was not certified by peer review) is the author/funder, who has granted bioRxiv a license to display the preprint in perpetuity. It is made available under aCC-BY 4.0 International license.

Supplementary Table 1 continued

	Cotylurus marcogliesei			*Alaria americana*		
	13,815 bp (52,172 reads)			**13,856 bp (117,847 reads)**		
Mitochondrial DNA				**start**	**stop**	**length**
cox3	1	655	655	1	655	655
trnH(gtg)	683	747	65	690	752	63
cob	751	1,875	1,125	756	1,883	1,128
nad4l	1,860	2,123	264	1,868	2,131	264
nad4	2,084	3,382	1,299	2,092	3,390	1,299
trnQ(ttg)	3,382	3,445	64	3,406	3,473	68
trnF(gaa)	3,468	3,533	66	3,477	3,544	68
trnM(cat)	3,541	3,609	69	3,554	3,624	71
atp6	3,613	4,131	519	3,628	4,146	519
nad2	4,151	5,041	891	4,142	5,056	915
trnV(tac)	5,045	5,107	63	5,060	5,121	62
trnA(tgc)	5,119	5,182	64	5,128	5,190	63
trnD(gtc)	5,196	5,261	66	5,198	5,266	69
nad1	5,271	6,170	900	5,273	6,187	915
trnP(tgg)	6,172	6,235	64	6,178	6,241	64
trnN(gtt)	6,245	6,300	56	6,249	6,312	64
trnI(gat)	6,311	6,376	66	6,334	6,399	66
trnK(ctt)	6,380	6,446	67	6,406	6,473	68
nad3	6,447	6,803	357	6,478	6,834	357
tRNA-Ser	6,803	6,862	60	6,846	6,905	60
trnW(tca)	6,869	6,933	65	6,914	6,973	60
cox1	6,942	8,552	1,611	6,983	8,620	1,638
tRNA-Thr	8,563	8,623	61	8,637	8,695	59
trnT(tgt)						
large subunit rRNA	8,627	9,614	988	8,689	9,694	1,006
trnC(gca)	9,615	9,679	65	9,695	9,760	66
rrnS	9,677	10,404	728	9,758	10,496	739
cox2	10,430	11,038	609	10,522	11,148	627
nad6	11,038	11,496	459	11,152	11,613	462
trnY(gta)	11,516	11,581	66	11,623	11,687	65
trnL1(aag)	11,587	11,650	64	11,694	11,759	66
trnS2(tga)	11,651	11,717	67	11,760	11,826	67
trnL2(taa)	11,723	11,787	65	11,885	11,950	66
trnR(tcg)	11,819	11,885	67	11,995	12,061	67
nad5	11,886	13,478	1,593	12,062	13,651	1,590
trnE(ttc)	13,483	13,548	66			
trnG(tcc)	13,748	13,812	65	13,767	13,833	67

Nuclear rDNA operon	**7761 bp (540,219 reads)**			**8240 bp (213,367 reads)**		
external transcribed spacer	1	468	468	1	1,007	1,007
small subunit rRNA	469	2,446	1,978	1,008	2,985	1,978
internal transcribed spacer 1	2,447	3,086	640	2,986	3,561	576
5.8S rRNA	3,087	3,243	157	3,562	3,718	157
internal transcribed spacer 2	3,244	3,534	291	3,719	4,013	295
large subunit rRNA	3,535	7,744	4,210	4,014	8,223	4,210
external transcribed spacer	7,745	>7761	>17	8,224	>8240	>17

bioRxiv preprint doi: https://doi.org/10.1101/333518; this version posted May 30, 2018. The copyright holder for this preprint (which was not certified by peer review) is the author/funder, who has granted bioRxiv a license to display the preprint in perpetuity. It is made available under aCC-BY 4.0 International license.

Supplementary Table 1 continued. Positions or anticodons of tRNAs in bold differ from those in other diplostomoids

	Hysteromorpha triloba				***Cyathocotyle prussica***				***Cardiocephaloides medioconiger***			
	13,855 bp (23,049 reads)				**13,665 bp (15,199 reads)**				**15,107 bp (144,789 reads)**			
Mitochondrial DNA	**start**	**stop**	**length**		**start**	**stop**	**length**		**start**	**stop**	**length**	
cox3	1	655	655		1	645	645		1	650	650	
trnH(gtg)	680	750	71		648	712	65		684	746	63	
cob	754	1,872	1,119		714	1,829	1,116		750	1,874	1,125	
nad4l	1,865	2,128	264		1,810	2,085	276		1,859	2,122	264	
nad4	2,089	3,384	1,296		2,046	3,332	1,287		2,083	3,387	1,305	
trnQ(ttg)	3,391	3,451	61		3,345	3,406	62		3,409	3,472	64	
trnF(gaa)	3,461	3,521	61		3,410	3,472	63		3,482	3,541	60	
trnM(cat)	3,528	3,597	70		3,478	3,541	64		3,586	3,653	68	
atp6	3,601	4,119	519		3,545	4,060	516		3,657	4,175	519	
nad2	4,115	5,110	996		4,069	4,965	897		4,171	5,082	912	
trnV(tac)	5,028	5,088	61	**trnA(tgc)**	4,988	5,052	65	**trnV(tac)**	5,091	5,154	64	
trnA(tgc)	5,101	5,168	68	**trnV(tac)**	5,067	5,130	64	**trnA(tgc)**	5,180	5,241	62	
trnD(gtc)	5,174	5,240	67		5,137	5,198	62		5,253	5,315	63	
nad1	5,244	6,170	927		5,199	6,092	894		5,319	6,230	912	
trnP(tgg)	6,156	6,218	63	**trnN(gtt)**	6,119	6,181	63	**trnP(tgg)**	6,243	6,309	67	
trnN(gtt)	6,231	6,292	62	**trnP(tgg)**	6,188	6,251	64	**trnN(gtt)**	6,318	6,382	65	
trnI(gat)	6,296	6,361	66		6,253	6,318	66		6,407	6,472	66	
trnK(ctt)	6,364	6,429	66		6,334	6,400	67		6,484	6,553	70	
nad3	6,433	6,789	357		6,403	6,750	348		6,555	6,911	357	
tRNA-Ser	6,793	6,852	60		6,758	6,815	58		6,950	7,015	66	
trnW(tca)	6,856	6,921	66		6,817	6,883	67		7,022	7,088	67	
cox1	6,933	8,570	1,638		6,888	8,438	1,551		7,162	8,724	1,563	
tRNA-Thr	8,589	8,658	70		8,447	8,511	65		8,741	8,803	63	
trnT(tgt)	8,589	8,655	67									
large subunit rRNA	8,659	9,652	994		8,515	9,506	992		8,794	9,835	1,042	
trnC(gca)	9,654	9,720	67		9,507	9,570	64		9,795	9,860	66	
rrnS	9,718	10,451	734		9,567	10,301	735		9,859	10,584	726	
cox2	10,477	11,097	621		10,327	10,920	594		10,611	11,219	609	
nad6	11,109	11,570	462		10,904	11,368	465		11,224	11,682	459	
trnY(gta)	11,584	11,647	64		11,370	11,434	65	**trnS2(tga)**	11,776	11,841	66	
trnL1(tag)	11,652	11,715	64	**trnL1(tag)**	11,444	11,508	65	**trnY(gta)**	12,615	12,678	64	
trnS2(tga)	11,716	11,781	66		11,506	11,574	69	**trnL2_1(caa)**	12,700	12,766	67	
trnL2(taa)	11,819	11,886	68		11,585	11,650	66		12,814	12,876	63	
trnR(tcg)	11,908	11,974	67		11,685	11,753	69		12,883	12,950	68	
nad5	11,973	13,565	1,593		11,753	13,339	1,587		12,951	14,546	1,596	
trnE(ttc)	13,572	13,635	64		13,347	13,407	61		14,559	14,624	66	
trnG(tcc)	13,781	13,852	72		13,596	13,662	67		15,032	15,105	74	
Nuclear rDNA operon	**8020 bp (640,736 reads)**				**8041 bp (51,101 reads)**				**7991 bp (286,106 reads)**			
external transcribed spacer	1	770	770		1	680	680		1	729	729	
small subunit rRNA	771	2,748	1,978		682	2,670	1,989		730	2,695	1,966	
internal transcribed spacer 1	2,749	3,341	593		2,671	3,338	668		2,696	3,312	617	
5.8S rRNA	3,342	3,498	157		3,339	3,495	157		3,313	3,469	157	
internal transcribed spacer 2	3,499	3,793	295		3,496	3,824	329		3,470	3,762	293	
large subunit rRNA	3,794	8,003	4,210		3,825	8,024	4,200		3,763	7,974	4,212	
external transcribed spacer	8,004	>8020	>17		8,025	>8041	>17		7,975	>7991	>17	

Supplementary Table 2. Selected morphometrics from adults of *Posthodiplostomum* reported in µm as range (mean, ± standard deviation, n)

Identification (present study)	***Posthodiplostomum centrarchi***		***P. centrarchi* and/or *Posthodiplostomum minimum***	
Identification (original source)			***P. minimum centrarchi,* and/or *P. minimum minimum***	
Source	**present study**		**Dubois, 1968**	
Life stage	**adult**		**adult**	
Host	***Ardea herodias***			
Locality	**Montreal, Quebec, Canada**			
	Length	**Width**	**Length**	**Width**
Body	1222 - 1775 (1518, ±186, 9)		890 - 1700	
Forebody	680 - 1200 (911, ±165, 9)	452 - 875 (622, ±130, 9)	540 - 1150	250 - 600
Hindbody	520 - 875 (639, ±108, 9)	248 - 750 (373, ±159, 9)	300 - 600	160 - 470
Forebody/Hindbody	0.58 - 0.86 (0.71, ±0.09, 9)		0.41 - 0.83	
Oral sucker	38 - 72 (52, ±10, 8)	38 - 72 (56, ±10, 8)	30 - 66	30 - 60
Pharynx	40 - 53 (49, ±4, 8)	40 - 53 (42, ±5, 8)	26 - 53	24 - 47
Oesophagus	60 - 72 (66, ±8, 2)		25 - 90	
Ventral sucker	55 - 90 (76, ±11, 9)	55 - 80 (71, ±8, 7)	42 - 95	50 - 100
VS position % in forebody	54 - 71 (60, ±6, 7)		60 - 71	
Tribocytic organ	140 - 200 (178, ±22, 8)	144 - 256 (195, ±44, 6)	125 - 220	125 - 190
Ovary	80 - 105 (92, ±11, 4)	72 - 88 (80, ±6, 4)	35 - 100	42 - 116
Anterior testis	96 - 200 (159, ±33, 7)	144 - 272 (204, ±49, 7)	70 - 170	120 - 240
Posterior testis	176 - 350 (257, ±58, 8)	216 - 350 (280, ±43, 9)	70-240	170-330
Eggs	70 - 98 (84, ±11, 10)	42 - 64 (56, ±8, 10)	73 - 91	48 - 64
N eggs	0 - 4 (1, ±1.7, 9)		≤8	
Copulatory bursa	120 - 216 (177, ±37, 8)	135 - 300 (248, ±55, 9)	145 - 160	

bioRxiv preprint doi: https://doi.org/10.1101/333518; this version posted May 30, 2018. The copyright holder for this preprint (which was not certified by peer review) is the author/funder, who has granted bioRxiv a license to display the preprint in perpetuity. It is made available under aCC-BY 4.0 International license.

Supplementary Table 3. Selected morphometrics from adults of *Cardiocephaloides medioconiger* reported in µm as range (mean, ± standard deviation, n)

Identification	*Cardiocephaloides medioconiger*		*C. medioconiger*	
Source	present study		Dubois, 1968	
Life stage	adult		adult	
Host(s)	*Thallassius maximus*			
Locality	Tavernier, Florida, USA			
	Length	Width	Length	Width
Body	7273 - 8324 (7832, ±529, 3)		4450 - 9000	
Forebody (FB)	1333 - 1616 (1468, ±142, 3)	1414 - 1455 (1431, ±21, 3)	630 - 1500	450 - 1360
Hindbody (HB)	5657 - 6869 (6364, ±631, 3)	1232 - 1293 (1266, ±31, 3)	2130 - 7500	500 - 1400
HB/FB	3.5 - 4.9 (4.4, ±0.8, 3)		2.5 - 5	
Oral sucker	103 - 160 (136, ±29, 3)	175 - 193 (187, ±10, 3)	81 - 179	75 - 136
Pharynx	129 - 152 (144, ±13, 3)	119 - 152 (136, ±17, 3)	66 - 183	66 - 192
Ventral sucker	103 - 168 (138, ±33, 3)	112 - 128 (120, ±8, 3)	104 - 157	75 - 138
Testicular zone	828 - 1010 (935, ±95, 3)		520 - 1200	
Anterior testis	303 - 475 (394, ±86, 3)		240 - 560	500 - 750
Posterior testis	363 - 484 (430, ±62, 3)	485 - 707 (599, ±111, 3)	285 - 578	500 - 750
Ovary	363 - 363 (363, ±0, 2)	300 - 363 (332, ±45, 2)	150 - 278	217 - 300
Eggs	94 - 117 (104, ±7, 12)	62 - 70 (68, ±3, 12)	96 - 131	63 - 78
Egg wall width	2 - 2.2 (2.1, ±0.1, 3)		2 - 4*	
Copulatory bursa (CB)	1010 - 1919 (1488, ±456, 3)		600 - 1600	
HB/CB	3.6 - 5.6 (4.5, ±1, 3)		3.3 - 8	

* see key to species of *Cardiocephaloides* p. 178, in Dubois (1968).

bioRxiv preprint doi: https://doi.org/10.1101/333518; this version posted May 30, 2018. The copyright holder for this preprint (which was not certified by peer review) is the author/funder, who has granted bioRxiv a license to display the preprint in perpetuity. It is made available under aCC-BY 4.0 International license.

Supplementary Table 4. Selected morphometrics from adults of *Cotylurus* reported in µm as range (mean, ± standard deviation, n)

Identification	*Cotylurus marcogliesei* n. sp.		*Cotylurus brevis*	
Source	present study		Dubois, 1968	
Life stage	adult		adult	
Host(s)	*Lophodytes cucullatus*			
Locality	Montreal, QC, Canada			
	Length	Width	Length	Width
Body	816 - 1152 (990, ±114, 8)		1000 - 1800	
Forebody	216 - 408 (313, ±51, 9)	312 - 640 (447, ±105, 8)	300 - 720	300 - 540
Hindbody	600 - 880 (722, ±100, 8)	256 - 520 (331, ±88, 7)	540 - 1110	260 - 660
Hindbody/Forebody	2.1 - 2.8 (2.3, ±0.2, 8)		1.25 - 1.94	
Oral sucker	48 - 80 (68, ±13, 8)	64 - 112 (86, ±14, 8)	72 - 120	61 - 120
Pharynx	30 - 50 (38, ±11, 3)		50 - 59	36 - 45
Ventral sucker	80 - 128 (107, ±18, 5)	96 - 168 (116, ±30, 5)	83 - 180	66 - 170
Anterior testis	136 - 168 (152, ±23, 2)		135 - 295	180 - 320
Posterior testis	136 - 160 (148, ±17, 2)		160 - 340	180 - 315
Ovary			75 - 150	65 - 120
N eggs	7 - 13 (10, ±3, 7)		"peu nombreux"	
Eggs	84 - 105 (94, ±7, 33)	38 - 65 (56, ±8, 33)	88 - 110	50 - 70
Genital bulb	104 - 144 (126, ±15, 5)	74 - 160 (112, ±32, 5)		
% extremity of antierior testis	40 - 45 (43, ±4, 2)			
% extremity of posterior testi	59 - 67 (63, ±4, 3)			

bioRxiv preprint doi: https://doi.org/10.1101/333518; this version posted May 30, 2018. The copyright holder for this preprint (which was not certified by peer review) is the author/funder, who has granted bioRxiv a license to display the preprint in perpetuity. It is made available under aCC-BY 4.0 International license.

Supplementary Table 5. Selected morphometrics from adults of *Alaria* reported in µm as range (mean, ± standard deviation, n)

Identification	*Alaria americana*		*Alaria americana*		*Alaria americana* (= *Alaria canis*)	
Source	present study		sources cited in Johnson, 1968		Larue and Fallis, 1936	
Life stage	adult		adult		adult	
Host(s)	*Vulpes vulpes*		*Canis familiaris, Vulpes fulva*		*Canis familiaris*	
Locality	Montreal, QC, Canada					
	Length	Width	Length	Width	Length	Width
Body	2121 - 2868 (2337, ±275, 7)		1160 - 4200		2500 - 4200 (3200)	
Forebody (FB)	1375 - 1858 (1510, ±177, 7)	465 - 869 (592, ±153, 6)			1600 - 2600 (2200)	680-950 (800)
Hindbody (HB)	606 - 1010 (815, ±124, 8)	252 - 559 (458, ±99, 7)			680 - 1600 (1000)	750 - 1100 (920)
FB/HB	1.8 - 2.3 (1.9, ±0.24, 7)		1.4 - 2.2			
Lappet	136 - 240 (190, ±38, 5)					
Oral sucker (OS)	64 - 120 (89, ±20, 5)	50 - 119 (82, ±27, 5)	75 - 140	75 - 150	75 - 140 (100)	110 - 150 (120)
Pharynx (PH)	120 - 150 (134, ±11, 6)	45 - 96 (81, ±20, 6)	120 - 196	80 - 153	140 - 170 (150)	90 - 140 (120)
OS/PH	0.49 - 0.83 (0.66, ±0.14, 5)		0.67			
Ventral sucker	88 - 104 (95, ±6, 6)	88 - 120 (101, ±11, 6)	70 - 176	90 - 140	90 - 120 (110)	90 - 140 (110)
Tribocytic organ	667 - 788 (736, ±40, 6)	160 - 250 (218, ±40, 4)				
Ovary	67 - 160 (105, ±37, 5)	65 - 280 (172, ±92, 4)				
Anterior testis	110 - 319 (219, ±91, 4)	120 - 327 (228, ±104, 3)				
Posterior testis	80 - 283 (165, ±79, 5)	152 - 270 (228, ±66, 3)				
Ejaculatory pouch	250 - 444 (346, ±70, 8)	101 - 135 (119, ±10, 8)				
Ejaculatory pouch wall		31 - 55 (42, ±7, 8)		35 - 55		
Eggs	102 - 136 (117, ±8, 25)	36 - 80 (64, ±8, 25)	90 - 133	64 - 86	108 - 116 (113)	64 - 76 (70)
N eggs	0 - 11 (7, ±4, 8)					

bioRxiv preprint doi: https://doi.org/10.1101/333518; this version posted May 30, 2018. The copyright holder for this preprint (which was not certified by peer review) is the author/funder, who has granted bioRxiv a license to display the preprint in perpetuity. It is made available under aCC-BY 4.0 International license.

Supplementary Table 6. Selected morphometrics from metacercariae and adults of *Hysteromorpha* from the present and other studies, reported in µm as range (mean, ± standard deviation, n)

	Hysteromorpha triloba				***Hysteromorpha corti***					
Identification	***H. triloba***		(***Diplostomum trilobum***)		***H. corti***		(***Hysteromorpha triloba***)		(***Diplostomulum corti***)	
Source	**present study**		**Ciurea, 1930**		**present study**		**Sereno-Uribe et al. 2018**		**Hughes, 1929**	
Life stage	**Metacercaria**		**Metacercaria**		**Metacercaria**		**Metacercaria**		**Metacercaria**	
Host(s)	***Squalius cephalus***		***Tinca tinca, Blicca bjoerkna, Idus idus, Rutilus rutilus***		***Notemigonus crysoleucas*** , ***Catostomus commersoni***		***Astyanax mexicanus***		***Ameiurus melas, A. nebulosus***	
Locality	**Italy**		**Danube region**		**St. Lawrencer River, Montreal, Canada; Lake Tarpon, Tampa, Florida**		**San Luis Potosi, Mexico**		**Illinois River, USA**	
	Length	**Width**	**Length**	**Width**	**Length**	**Width**	**Length**	**Width**	**Length**	**Width**
Body	776 - 889 (830 ±42, 7)		690 - 1250		712 - 880 (797 ±55, 7)		641 - 836 (736)		700 - 880 (810, 4)	
Forebody	536 - 664 (606 ±48, 7)	576 - 687 (630 ±33, 7)	460 - 860	420 - 690	640 - 696 (670 ±25, 5)	384 - 472 (429 ±34, 7)	453 - 586 (547)	498 - 532 (517)		400 - 530 (475, 4)
Pseudosucker	48 - 80 (64 ±12, 7)	44 - 96 (69 ±14, 12)	70 - 110 diameter				57 - 90 (71)	45 - 66 (53)		
Hinbody	120 - 303 (225 ±62, 7)	256 - 545 (404 ±96, 7)	200 - 400	260 - 390	80 - 160 (126 ±32, 5)	152 - 200 (176 ±34, 2)	136 - 251 (188)	209 - 349 (289)		
Oral sucker	72 - 125 (82 ±19, 7)	52 - 84 (70 ±12, 7)	66 - 96 diameter		60 - 68 (62 ±4, 5)	56 - 68 (63 ±4, 5)	56 - 65 (61)	43 - 56 (52)	62 - 72 (67, 4)	
Pharynx	50 - 76 (61 ±10, 7)	30 - 44 (36 ±4, 7)	55 - 73	39 - 50	32 - 35 (33 ±2 3)	32 - 35 (33 ±2, 3)	42 - 53 (48)	24 - 35 (55?)	40 - 53 (45, 3)	26 - 38 (33, 3)
Oesoaphagus	20 - 47 (34 ±19, 2)		18 - 48						15 - 21 (19, 4)	
Ventral sucker	60 - 82 (70 ±8, 7)	88 - 107 (99 ±6, 7)	77 - 120 diameter		56 - 68 (60 ±6, 5)	60 - 76 (73 ±6, 6)	47 - 54 (50)	69 - 76 (72)	73 - 83 (76, 4)	
Tribocytic organ	160 - 229 (193 ±27, 6)	163 - 320 (207 ±54, 7)	200 - 330	120 - 290	136 - 176 (163 ±18, 4)	116 - 160 (137 ±19, 5)	143 - 195 (179)	134 - 158 (146)		

Identification	(***Hemistomum trilobum***)*		(***Diplostomum trilobum***)		***H. corti***		(***Hysteromorpha triloba***)	
Source	**Krause, 1915**		**Ciurea, 1930**		**present study**		**Sereno-Uribe et al. 2018**	
Life stage	**Adult**		**Adult**		**Adult**		**Adult**	
Host(s)	***Phalacrocorax carbo***		***Phalacrocorax carbo***		***Phalacrocorax auritus***		***Phalacrocorax brasilianus***	
Locality	**Europe**		**Eastern Europe**		**Montreal, Quebec, Canada**		**La Angostura, Chiapas, Mexico**	
	Length	**Width**	**Length**	**Width**	**Length**	**Width**	**Length**	**Width**
Body	780 - 840		780 - 1910		1052 - 1633, 1314±172, 12		1068 - 1333 (1220)	
Forebody	470 - 690	470 - 500	390 - 690	390 - 1050	490 - 762, 664±86, 12	404 - 707, 509±82, 12	441 - 616 (558)	566 - 754 (665)
Pseudosucker			55 - 170 diameter		47 - 129, 78±26, 9	70 - 200, 105±38, 9	82 - 108	90 - 168
Hindbody	130 - 360		390 - 1210	340 - 620	490 - 943, 658±125, 12	381 - 636, 480±68, 12	534 - 731 (657)	407 - 540 (465)
Oral sucker	68		77 - 130 diameter		50 - 107, 75±16, 12	71 - 107, 86±12, 12	72 - 88 (80)	77 - 95 (86)
Pharynx	45 - 49	36 - 40	55 - 88	37 - 57	36 - 71, 53±12, 12	36 - 70, 51±10, 12	47 - 70 (56)	40 - 51 (45)
Ventral sucker	81 - 117	90 - 110	111 - 167 diameter		36 - 107, 75±18, 11	43 - 143, 93±30, 11	80 - 100 (90)	90 - 109 (98)
Tribocytic organ	215 - 275		220 - 340	170 - 380	142 - 321, 241±58, 12	190 - 293, 237±33, 11	184 - 376 (286)	248 - 490 (337)
Ovary			40 - 120	100 - 240	71 - 100, 85±14, 5	64 - 114, 81±19, 5	104 - 179 (140)	75 - 156 (105)
Anterior testis			120 - 290	120 - 230	107 - 214, 169±31, 10	107 - 250, 171±48, 7	130 - 194 (172)	134 - 227 (194)
Posterior testis			80 - 240	280 - 490	143 - 229, 171±35, 9	357 - 500, 423±51, 8	136 - 369 (201)	179 - 455 (366)
Eggs	81	54	91 - 99	55 - 62	87 - 109, 98±6, 12	44 - 66, 54±6, 12	77 - 98 (85)	46 - 83 (55)

*redescription of type specimens

bioRxiv preprint doi: https://doi.org/10.1101/333518; this version posted May 30, 2018. The copyright holder for this preprint (which was not certified by peer review) is the author/funder, who has granted bioRxiv a license to display the preprint in perpetuity. It is made available under aCC-BY 4.0 International license.

Supplementary Table 7. Selected morphometrics from adults of *Tylodelphys immer* reported in µm as range (mean, ± standard deviation, n)

Identification	*Tylolephys immer*		*Tylolephys immer*	
Source	present study		Dubois, 1968	
Life stage	adult		adult	
Host(s)	*Gavia immer*			
Locality	Montreal, QC, Canada			
	Length	Width	Length	Width
Body	1515 - 1636 (1592, ±50, 5)		1470 - 1840	
Forebody (FB)	970 - 1111 (1046, ±58, 5)	455 - 556 (507, ±44, 5)	690 - 1140	320 - 580
Hindbody (HB)	525 - 566 (545, ±15, 5)	284 - 404 (352, ±46, 5)	330 - 790	220 - 470
HB/FB	0.47 - 0.56 (0.52, ±0.04, 5)		0.45 - 0.76	
Lappet	160 - 232 (197, ±19, 5)		180 - 280	
Oral sucker	80 - 119 (102, ±15, 5)	100 - 127 (114, ±13, 5)	72 - 120	80 - 115
Pharynx	68 - 84 (79, ±6, 5)	66 - 80 (73, ±5, 5)	60 - 89	48 - 70
Ventral sucker	90 - 109 (100, ±8, 5)	100 - 131 (114, ±12, 5)	70 - 100	80 - 122
Tribocytic organ	240 - 288 (262, ±24, 5)	152 - 240 (192, ±32, 5)	190 - 270	100 - 210
Ovary	40 - 80 (61, ±20, 3)	56 - 80 (69, ±12, 3)	95 - 115	80 - 145
Anterior testis	80 - 96 (88, ±7, 4)	272 - 344 (310, ±30, 4)	90 - 200	250 - 380
Posterior testis	88 - 112 (102, ±10, 5)	272 - 320 (294, ±22, 5)	90 - 195	215 - 350
Eggs	80 - 100 (93, ±7, 12)	40 - 68 (54, ±8, 12)	83 - 104	54 - 68
N eggs	1 - 8 (5, ±3, 5)		3 - 17	

bioRxiv preprint doi: https://doi.org/10.1101/333518; this version posted May 30, 2018. The copyright holder for this preprint (which was not certified by peer review) is the author/funder, who has granted bioRxiv a license to display the preprint in perpetuity. It is made available under aCC-BY 4.0 International license.